

Assignment of Direct vs. Indirect Mechanisms Used by Fungi for Polyurethane Coating Degradation

SERDP Final Report for SEED WP-2745

Principal Investigator: Justin C. Biffinger, PhD (University of Dayton; jbiffinger1@udayton.edu)

Co-PI: Wendy J. Crookes-Goodson, PhD (AFRL)

NRL Team Lead: Daniel E. Barlow, PhD (NRL)

5/31/2018

Version 1s

REPORT DOCUMENTATION PAGE

*Form Approved
OMB No. 0704-0188*

The public reporting burden for this collection of information is estimated to average 1 hour per response, including the time for reviewing instructions, searching existing data sources, gathering and maintaining the data needed, and completing and reviewing the collection of information. Send comments regarding this burden estimate or any other aspect of this collection of information, including suggestions for reducing the burden, to Department of Defense, Washington Headquarters Services, Directorate for Information Operations and Reports (0704-0188), 1215 Jefferson Davis Highway, Suite 1204, Arlington, VA 22202-4302. Respondents should be aware that notwithstanding any other provision of law, no person shall be subject to any penalty for failing to comply with a collection of information if it does not display a currently valid OMB control number.
PLEASE DO NOT RETURN YOUR FORM TO THE ABOVE ADDRESS.

1. REPORT DATE (DD-MM-YYYY) 05/31/2018		2. REPORT TYPE SERDP Final Report		3. DATES COVERED (From - To)	
4. TITLE AND SUBTITLE Assignment of Direct vs. Indirect Mechanisms Used by Fungi for Polyurethane Coating Degradation				5a. CONTRACT NUMBER WP-2745	
				5b. GRANT NUMBER	
				5c. PROGRAM ELEMENT NUMBER	
6. AUTHOR(S) Justin C. Biffinger, Wendy J. Crookes-Goodson, Daniel E. Barlow				5d. PROJECT NUMBER WP-2745	
				5e. TASK NUMBER	
				5f. WORK UNIT NUMBER	
7. PERFORMING ORGANIZATION NAME(S) AND ADDRESS(ES) Air Force Research Laboratory Wright-Patterson Air Force Base Dayton, OH 45433				8. PERFORMING ORGANIZATION REPORT NUMBER WP-2745	
9. SPONSORING/MONITORING AGENCY NAME(S) AND ADDRESS(ES) Strategic Environmental Research and Development Program 4800 Mark Center Drive, Suite 17D03 Alexandria, VA 22350-3605				10. SPONSOR/MONITOR'S ACRONYM(S) SERDP	
				11. SPONSOR/MONITOR'S REPORT NUMBER(S) WP-2745	
12. DISTRIBUTION/AVAILABILITY STATEMENT Distribution A; unlimited public release					
13. SUPPLEMENTARY NOTES Performing Organization includes University of Dayton and U.S. Naval Research Laboratory					
14. ABSTRACT Fungi can survive on any polyurethane coating if oxygen and moisture are present resulting in the deterioration of protective coatings and, potentially, of the supporting weapon system structure. This is a systemic problem for sustaining our fleet and providing a safe environment to our military personnel. The objective of this SEED program was to correlate the biodegradation of polyurethane coatings to the physiological and chemical real-time responses of fungi isolated and identified from coatings inside of active aircraft.					
15. SUBJECT TERMS Fungi, Polyurethane Coatings, Aircraft Coatings, Biodegradation					
16. SECURITY CLASSIFICATION OF:			17. LIMITATION OF ABSTRACT	18. NUMBER OF PAGES	19a. NAME OF RESPONSIBLE PERSON
a. REPORT	b. ABSTRACT	c. THIS PAGE			Justin Biffinger
UNCLASS	UNCLASS	UNCLASS	UNCLASS	47	19b. TELEPHONE NUMBER (Include area code) 860-906-8301

**PUBLIC AFFAIRS SECURITY AND POLICY
REVIEW WORKSHEET**

(See reverse for instructions)

* 1. DATE NEEDED

30 Mar 18

2. SUBMITTER REFERENCE NO.

RX18-0215

NOTE: Application to clear information for Public Release. Public release clearance is NOT required for material presented in a closed meeting and which will not be made available to the general public, on the Internet, in print or electronic media. **Items marked with an asterisk (*) and Blocks 12-14 are required.**

3. SUBMITTER

*NAME
 *PHONE ORG/OFC SYM
 *EMAIL
 *ORG. EMAIL

4. PRIMARY AUTHOR

*NAME
 *PHONE
 *ORG/OFC SYM
 *EMAIL

*5. DOCUMENT TITLE

*6. CONFERENCE/EVENT/PUBLICATION/WEBSITE/PUBLIC WEB URL

*7. EVENT/PUBLICATION DATE

*8. DOCUMENT TYPE

OTHER

*9. BUDGET CATEGORIES (Choose N/A if not applicable)

OTHER

10. NATIONAL SECURITY STATUTES/TECHNOLOGY ISSUES

*a. Are any aspects of this technology included in: U.S. Munitions List; ITAR 22, CFR Part 121; CCL; Program Protection Plan, Security Classification Guide?
 (If YES, please explain rationale for release in block 11)

YES NO

*b. Does this information meet the criteria for Public Release - unclassified, unlimited distribution?

YES NO

*c. Are any references classified or subject to distribution limitations?
 (If YES, please explain rationale for release in block 11)

YES NO

*d. If this material results from an international agreement, is the DoD authorized to release program information?
 (If NO, identify release authority organization in block 11)

YES NO N/A

*e. If this is a joint program, does your organization maintain primary management responsibility and authority to release all information?
 (If NO, provide name of lead organization/POC [i.e. DARPA, NASA, Army, Navy, etc.] in block 11)

YES NO N/A

11. EXPLANATION (Additional comments, previous related cases [include case number], additional coordination accomplished/required. Instructions on reverse)

CERTIFICATION AND COORDINATION SIGNATURES. SIGNATURES MAY NOT BE REPEATED IN MULTIPLE BLOCKS.
 NOTE: PER REGULATORY GUIDANCE, **CONTRACTORS MAY NOT SIGN IN BLOCKS 12-15**

12. DoD ORIGINATOR/PROGRAM MANAGER (Required)

I certify the attached material is unclassified, technically accurate, contains no critical military technology, is not subject to export controls and is suitable for public release.

NAME
 ORG OFC SYMBOL
 SIGNATURE Digitally signed by MEADE.MITCHELL.LEE.1362279409
 Date: 2018.03.09 14:09:01 -05'00'
 DUTY TITLE DATE

13. TECHNICAL REVIEW AND CERTIFICATION (Required)

I certify the information contained in the attached document is technically accurate; does not disclose classified, sensitive, or militarily critical technology; does not violate proprietary rights or copyright restrictions, and is not subject to export control regulations. I certify that this information is suitable for public release.

NAME
 ORG OFC SYMBOL
 SIGNATURE Digitally signed by SOWARDS.LAURA.A.1073905148
 Date: 2018.03.12 11:15:42 -04'00'
 DUTY TITLE DATE

14. SECURITY MANAGER REVIEW (Required)

I certify that the information has been reviewed and the information contains no Operational Security or foreign disclosure issues.

NAME
 ORG OFC SYMBOL
 SIGNATURE Digitally signed by KLUG.KEITH.BRIAN.1163567128
 Date: 2018.03.13 08:13:28 -04'00'
 DUTY TITLE DATE

15. ADDITIONAL REVIEW (See reverse for instructions)

I certify that this information is suitable for public release.

NAME
 ORG OFC SYMBOL
 SIGNATURE Digitally signed by RUSSELL.WILLIAM.E.JR.1007068057
 Date: 2018.03.12 15:15:42 -04'00'
 DUTY TITLE DATE

16. PA USE ONLY

NOTES:

- APPROVED
- AS AMENDED
- w/RECOMMENDATION
- OTHER (Annotate in notes)
- NO OBJECTION
- RETURN - NO ACTION
- NOT CLEARED
- OBJECTION

PUBLIC AFFAIRS OFFICER

Digitally signed by MITCHELL.JAMES.MARVIN.1081879520
 Date: 2018.05.30 10:02:45 -04'00'

CASE NUMBER

Block 11 - Explanation (Continued):

AF/A4 - No Objection 1 Apr 2018
AF/SG - No Objection 11 May 2018
DoD - No Objection 24 May 2018
SAF/PAO - No Objection 11 Apr 2018
Case Number: 2018-0248 (original case number(s): MSC/PA-2018-0046; 88ABW-2018-1328) The material was assigned a clearance of CLEARED on 24 May 2018
Closed in PA Information release system by SAF/PA on 24 May 2018

INSTRUCTIONS FOR COMPLETING THE SECURITY AND POLICY REVIEW WORKSHEET

NOTE: Items marked with an asterisk (*) and Blocks 12-14 are required. If all required information is not provided, case will be returned with no action taken and must be resubmitted.

1. Date Needed: Allow at least 10 working days (*not including day of submission*) for local PA review. If a submission requires higher level review or coordination, processing time could take up to 45 working days.
 - Requests for less than 10 working days require a justification letter as to why the submission does not fall within the required time frame signed by a Directorate-Level Director or Commander. More information including a justification letter template is available on the S&PR SharePoint Site.
 - Depending on complexity or requirements for other coordination, items can take longer to process (i.e. Theses) You will be notified of any issues.
 - Items already publicly presented will not be reviewed.
2. Include your organizational reference/tracking number (optional). Tracking numbers will not be added by PA.
3. Submitter information: Self explanatory. *These e-mail addresses receive notification when case is assigned and completed.*
4. Author(s) information: List primary author's name, if multiple authors. *This e-mail address receives notification when case is assigned and completed.*
5. Document Title: Self-explanatory.
6. Conference/Event/Publication Name/Website URL. Identify date of event/name of publication where submission will be published, or web site where cleared material will be posted.
7. Event/Publication Date: Identify date of event or date of publication/posting to web site.
8. Document type: Indicate the type of information to be reviewed from the pull down menu, or choose Other and fill in that blank.
9. Identify the budget category or program element code associated with the weapon system from pull down menu, or choose NA.
10. National Security Statutes/Technology Issues:
 - a. References:
 - [Electronic Code of Federal Regulations](#).
 - [Export Administration Regulations Database](#).
 - [U.S. Munitions List \(Part 121\)](#) and [International Traffic In Arms Regulations](#)
 - [The Commerce Control List](#)
 - b. Materials that must be/are marked FOUO or Distribution B or higher will not be cleared.
 - c. Identify whether classified references are used. Annotate in Block 11 (Explanation) exact references and why it is necessary to use them.
11. Explanation. Include additional comments from other blocks (list previous related cases), clearly identify coordination with agencies already accomplished. If additional coordination with other command agencies is required, provide POC information (use back of form, as necessary).

CERTIFICATION AND COORDINATION SIGNATURES. PER REGULATORY GUIDANCE, **CONTRACTORS MAY NOT SIGN IN BLOCKS 12-15**

12. Originator/Program Manager/Author Certification. Signature certifies that the U.S. Government originator, program manager, or author concurs that the information is appropriate for public release based on regulations, classification guides, and any other pertinent guidance.
13. Technical Review and Certification Signature. Signature certifies that the information has been reviewed by a U.S. Government superior/authorized peer reviewer/subject matter expert and is appropriate for public release based on regulations, classification guides, and any other pertinent guidance.
14. Security Manager Review. Signature certifies that the information contains no Operational Security issues. This can be signed by a U.S. Government OPSEC Officer, Security Manager (or Educational Department Head for theses, dissertations and abstracts).
15. Additional review. Used to document coordination with outside agencies/program offices, or organizations may have an internal process that requires an additional signature, such as director or commander. Required only when external coordination needs to be documented, or internal processes dictate additional review.

Contents

Abstract.....	1
Objective.....	3
Background.....	4
Materials and Methods.....	5
Results and Discussion	9
Conclusions and Implications for Future Research	34
Literature Cited.....	35
Appendix.....	38

List of Tables

Table 1 Differential peak positions from Figure 13d,e	22
Table 2 Comparison of carbon sources used for the growth of all fungi being studied for this program.....	26

List of Figures

Figure 1 Schematic of the three outcomes resulting from the interaction of a microorganism with a synthetic polymer coatings.....	10
Figure 2 Organizational chart for increasing the polymer resistance to degradation based on coating composition.....	11
Figure 3 Chemical structures of Polyethylene Succinate (PES), Polyethylene adipate (PEA), and Irogran [®] and the predicted hydrolysis products.....	12
Figure 4 Time-dependent production of CO ₂ by a) <i>Fungus 1</i> and b) <i>Fungus 2</i> from polyethylene succinate (PES), polyethylene adipate (PEA), Irogran [®] and from vials without polymer with cells (Glass (Control)) during biodegradation over 7 days.	12
Figure 5 Representative average chromatographs from three biological replicates from gas sampled from the headspace over the active biodegradation of polyethylene succinate (PES) at 1 day (orange) and 22 days (blue) by <i>Fungus 1</i> at 25°C.	13

Figure 6 Selected time-dependent phase contrast (Phase I) optical microscopy images of a region of a PEA coating exposed to *Fungus 1* or *Fungus 2* after the initial exposure (Day 0) and 2 and 7 days after exposure..... 14

Figure 7 Overlapping scanning confocal laser profile and optical images of PEA coatings exposed for 8 days to a) *Fungus 1* , c) *Fungus 2* . The lines rendered onto images a and c indicate where 2-point height profiles were extracted for b) *Fungus 1* (blue line), c) *Fungus 2* (red line) compared to sterile water (control) (grey line; from **Figure S1**. 15

Figure 8 Selected time-dependent phase contrast (Phase I) optical microscopy images of a region of a PES coating exposed to *Fungus 1* or *Fungus 2* after the initial exposure (Day 0) and 2 and 7 days after exposure..... 16

Figure 9 Overlapping scanning confocal laser profile and optical images of PES coatings exposed for 8 days to a) *Fungus 1*, c) *Fungus 2* . The lines rendered onto images a and c indicate where 2-point height profiles were extracted for b) *Fungus 1* (blue line), c) *Fungus 2* (red line) compared to sterile water (control) (grey line; from **Figure S2**)..... 17

Figure 10 Selected time-dependent phase contrast (Phase I) optical microscopy images of a region of a Irogran[®] coating exposed to *Fungus 1* or *Fungus 2* after the initial exposure (Day 0) and 2 and 7 days after exposure. The orange arrow shows the same cell mass as indicated in **Figure 12**. 18

Figure 11 Overlaid scanning confocal laser profile and optical images of Irogran[®] coatings exposed for 8 days to water-washed suspensions of a) *Fungus 1* , b) *Fungus 2* , or c) sterile water at RH: 100% at 25°C. Images were taken at the boundary of the drop of the original sample. Red scale bars set to 100 μm. The orange arrow shows the same cell mass as indicated in **Figure 10**. 19

Figure 12 Overlaid scanning confocal laser height profile and optical images of Irogran[®] coatings exposed for 8 days to a) *Fungus 1* and the b) resulting height profile from the rendered blue line on (a), c) *Fungus 2*, and the d) resulting height profile from the rendered red line on (c). Grey height profiles on (b) and (d) were calculated from sterile water results (control; **Figure S3**). 20

Figure 13 Infrared microscopy data from the biodegradation of Irogran[®] coatings (PU) on ZnSe windows using drop cast *Fungus 1* (PI) at 100% humidity (25°C). a) Optical image of *Fungus 1* drop-cast on Irogran[®] coating with spectra collected at the ‘+’ marks (b,c) Spectra collected on

and off the biofilm, respectively. Vertical arrows identify the 1735 cm⁻¹ and 1700 cm⁻¹ carbonyl peak and shoulder. (d) Difference spectrum for ‘b’ – ‘c’. Asterisks and daggers identify positive and negative peaks. (e) Difference spectrum collected by same procedure for *Fungus 2* on Irogran (f) Spectrum of *Fungus 1* biofilm on ZnSe with no polymer layer 21

Figure 14 Transmission micro FTIR spectra of (a) *Fungus 1* on PET1 polyether polyurethane film (b) adjacent biofilm free region of the polymer (c) difference spectrum..... 23

Figure 15 Raman depth slices acquired from a *Fungus 1* biofilm on a ~ 10 μm Irogran[®] film. The upper left figure shows an optical image at the top and depth slice data below. The optical image is viewing the underside of the biofilm through the polymer and the yellow line indicates the location the depth slice was acquired. 24

Figure 16 Normalized cell densities of 48 hours planktonic cultures of a) *Fungus 1* and b) *Fungus 2* in M9 media at either pH 7.5 or 5.5 with carbon sources potentially generated from the hydrolysis of PES, PEA, and Irogran[®] coatings or similar aliphatic polyester polyurethane coatings, and (c) Structure and naming of the carbon sources used for growth. 25

Figure 17 (Top) Optical images of a *Fungus 1* biofilm on an Irogran[®] film used for AFM-IR analysis. The images show the biofilms at 24 hours and after 25 days at 25°C and 100% relative humidity. (Bottom) AFM imaging showing changes occurring at the single cell level. 28

Figure 18 AFM-IR imaging showing varying local PU degradation by *Fungus 1* after 25 days at RH% = 100 30

Figure 19 Additional high PU degradation localized at single cells. 25 day time point..... 31

Figure 20 Localized degradative cracking and additional changes. (30 day time point.)..... 31

Figure 21 Comparison of the concentration of CO₂ generated by *Fungus 3* after 336 h on all polymers and an image of the degradation of Irogran[®] (left vial) by *Fungus 3* compared to the control vial with Irogran[®]. PES: Polyethylene succinate, PEA: Polyethylene adipate, Glass (control experiment with cells and no polymer). 32

Figure 22 Selected time-dependent phase contrast (Phase I) optical microscopy images of a region of a Polyethylene adipate coating exposed to *Fungus 3* over 3 days of exposure at RH: 100%. 33

Figure 23 Selected time-dependent phase contrast (Phase I) optical microscopy images of a region of a Irogran[®] coating exposed to *Fungus 3* over 14 days of exposure at RH: 100%. 33

Figure 24 Comparison of the concentration of CO₂ generated by *Fungus 4* after 336 h on all polymers and an image of the degradation of Irogran (left vial) by *Fungus 4* compared to the control vial with Irogran. PES: Polyethylene succinate, PEA: Polyethylene adipate, Glass (control experiment with cells and no polymer) 34

List of Acronyms

DoD	Department of Defense
JGI	DOE Joint Genomic Institute
AFRL	Air Force Research Laboratory (Wright Patterson Air Force Base)
NRL	Naval Research Laboratory (Washington, DC)
PU	Polyurethane
PL	<i>Papiliotrema laurentii</i>
NA	<i>Naganisha Albida</i>
PEA	Polyethylene adipate
PES	Polyethylene succinate
AFM	Atomic force microscopy
ATR	Attenuated Total Reflectance
DNA	deoxyribonucleic acid
TSB	Tryptic Soy Broth
RH	Relative Humidity
IR	Infrared Spectroscopy
FTIR	Fourier transfer Infrared Spectroscopy

Keywords: Biodegradation, Fungi, Polyurethane, Polyester

Acknowledgements: The authors acknowledge AFOSR program elements AFRL: 12RX14COR NRL: F4FGA05338G001 for additional support. We acknowledge the contribution of Abby Neal, John N. Russell Jr., Vanessa Varaljay, Carrie Drake, Bryan Crable, for input that overlaps with the AFOSR program.

Abstract

Objective: Fungi can survive on any polyurethane coating if oxygen and moisture are present resulting in the deterioration of protective coatings and, potentially, of the supporting weapon system structure. This is a systemic problem for sustaining our fleet and providing a safe environment to our military personnel. *The objective of this SEED program was to correlate the biodegradation of polyurethane coatings to the physiological and chemical real-time responses of fungi isolated and identified from coatings inside of active aircraft.*

Technical Approach: Our team performed experiments with two different fungal morphotypes using a total of 4 fungal species (*Fungus 1*, *Fungus 2*, *Fungus 3*, and *Fungus 4*) that were isolated from inside aircraft and were cultured/and screened against a colloidal polyester polyurethane (Impranil®DLN). These fungi were then challenged individually as biofilms on two polyesters (polyethylene succinate, polyethylene adipate), a polyurethane-based coating with polyester and polyether blocks (Irogran®; PS455-203), and ultimately with two polyether polyurethanes at two different relative humidity ranges (RH: 70% and 100%). The two different humidity levels were used to evaluate the role of water in the degradation process. These polyester and polyether polyurethane coatings were spin-coated and cured on silicon, quartz, or zinc selenide transparent substrates and then challenged with the fungal strains listed above as air-dried biofilms. Polyurethane biodegradation products and fungal biodegradation mechanisms for all polymers were determined using spatially and/or temporally resolved spectroscopy techniques and imaging including Raman and IR microscopies. Single-cell microscopy, characterization of localized polymer degradation, and the relationship between degradation and the fungal response were determined using atomic force microscopy (AFM)-IR techniques (NanoIR™) and 3D confocal microscopy. The potential metabolic responses as the coatings were degraded and their reaction to the potential hydrolysis products were compared using carbon dioxide production over time from biofilms and a growth screen based on planktonic optical density changes.

Results: Our team completed a comprehensive evaluation of two non-motile yeast strains (*Fungus 1* and *Fungus 2*) during the degradation of all polymers and started to compare those results to a fungal mold, *Fungus 3*, which was capable of spreading over the polymer surface during the degradation process. Our results confirm that we have isolated and characterized three new fungal strains that are capable of degrading polyester polyurethane coatings. Our success with identifying fungi capable of biodeterioration places our research team in the position to identify actual degradation pathways that are shared between non-motile yeasts and *Basidiomycetes*. Thus far, all fungi have hydrolyzed the soft polyester segments of these coatings and not the polyurethane nor polyether segments. Here are some specific highlights from our work so far.

- *Fungus 1* and *Fungus 2* were isolated from the inside of aircraft and cleared Impranil®DLN containing agar plates
- Biofilms of both strains metabolized polyethylene succinate, polyethylene adipate, and the polyester component of Irogran® to different degrees without additional carbon sources

- Carbon dioxide production in the headspace above polymer degradation experiments confirmed that both fungal strains were metabolically active while degrading the polymers
- *Fungus 1* and *Fungus 2* grew on and degraded PEA coatings rapidly while only *Fungus 1* grew and degraded PES coatings.
- *Fungus 1* degraded Irogran[®] to a greater degree than *Fungus 2* and infrared microscopy data confirmed that the soft polyester segment was hydrolyzed preferentially to the hard polyurethane segment
- Adipate was a viable carbon source for *Fungus 1* and *Fungus 2* biofilm growth on the polymer surface but not as a soluble carbon source for planktonic cultures.
- AFM-IR demonstrated non-homogenous Irogran[®] film degradation at the single cell level by *Fungus 1* biofilms. Aggregation and transport of degradation resistant polymer components was also revealed.
- The two remaining fungi designated for this SEED program, *Fungus 3* and *Fungus 4*, are capable of growing and degrading Irogran[®] but the mechanisms for degradation were not determined.

Benefits: Through this SEED program we have identified two new non-motile yeast strains (*Fungus 1* and *Fungus 2*) that are active degraders of polyurethane coatings from our active aircraft. We have isolated several polymer degrading organisms to date and have defined how moisture leads to the greatest difference in reactivity on all the coatings. Based on our data, both *Fungus 1* and *Fungus 2* are model organisms for studying and developing predictive biodegradation models for new alternative coating formulations and techniques. The activity of these yeasts indicates that they are direct degraders of the polyester coatings since they can both hydrolyze polyester based coatings and metabolize the hydrolysis products to CO₂; *i.e.* the polymer was considered a viable carbon source. *Fungus 1* and *Fungus 2* are ideal candidates for future studies as their attachment and degradation mechanisms in conjunction with their lack of motility results in predictable patterns of degradation (based on pitting by fungal generated secondary compounds) on any polymer surface. Our results also indicated that moisture is critical to the rapid degradation of the coatings; we observed no biodegradation below a relative humidity of 70%.

Thwarting biofilm and coating degradation is not a new area of study; however, we believe that research and development in this area is still guided by legacy compounds and concepts where cell death is more important than control over the microorganism. We cannot control when and if an organism will land on our weapon systems, we can only respond and adapt to what it does as a result of being on that surface. The more sensitive our solutions are to an organism's natural behavior, the more likely that a universal solution to coating biodegradation can be discovered.

Objective

While exposed to a coating, fungi are at adapting to a coating's composition and through degradation viable carbon source or potential poisons will be released that the fungi must resist. Thus, formulating new more environmentally friendly coatings that resist biodegradation depends heavily on predicting the result of these very fundamental interactions. Defining why a fungal strain degraded a coating needs to be analyzed at the earliest stages of the biodegradation process since it is the initial fungal response to the coating that will result in the greatest impact over thwarting biodegradation over the lifetime of the coating. Analyzing the degradation process after a fungal species or a consortium of microorganisms have started to grow over a coating surface is too late since cell death and lysis at later stages of biofouling will always create a barrier between any next generation antimicrobial agents in a coating regardless of its effectiveness.

The proof of concept for this SEED program was to correlate the biodegradation of DoD-relevant polyurethane coatings to the physiological and chemical real-time responses of fungi isolated and identified from coatings inside of active aircraft.

We analyzed two non-motile yeasts (*Fungus 1* and *Fungus 2*) initially since polymer degradation would occur without the active movement of the organisms which led to predictable degradation patterns on the coatings. We used these fungi to generate a baseline activity on all polymers. Not only did *Fungus 1* and *Fungus 2* provide this baseline but they clearly degraded the polymers differently. Our results also show that the role of water in the biodegradation process is intimately associated with the successful decomposition of polyester-based coatings by the cell. Our knowledge of these non-motile yeasts and improvements in our experimental design limits the risks associated with comparing different families of fungi since we have defined behaviors and identified that water and its movement is an essential variable to control and manipulate during the degradation process.

We have also performed all the proof-of-concept biofilm experiments and spectroscopy. This will allow us to now create larger arrays of data more quickly and potentially include metabolic staining with microscopy data. We have also started working with baseline transcriptional data from biofilms which is a starting point for a complete transcriptional profile focused on metabolism and activity at a polymer surface and throughout the coating degradation process. AFRL has also submitted genomic DNA from *Fungus 1* to JGI for complete sequencing and annotation which opens the possibility of taking all of the degradation results generated in the SEED program and comparing them to how *Fungus 1* was regulating certain classes of genes in response to water, polymer, the polymer degradation products. These fundamental transcriptional responses to the coatings based on the physical and degradation behavior we have observed in this SEED effort will lead our ultimate long-term goal of predicting fungal degradation behavior without screening every polymer formulation against the activity of every possible fungal strain. Our results thus far with *Fungus 3* and *Fungus 4* indicate that these fungi are more active polymer degraders compared to the non-motile yeast strains and that comparisons between *Fungus 3* and *Fungus 4* to the yeast strains will complete

our first pass at a unified mechanism for degradation between fungal strains. We are a team focused on the objective of defining when we can control the biodegradation of a polymer and not the microorganism. As new environmentally friendly alternative coatings are formulated, and anti-microbial additives are replaced with new compounds, our results will aid in decreasing the time toward application and increasing the effectiveness of the antimicrobial aspects of the coatings at the formulation stage.

Background

Polymer coatings and composites are essential to increasing the operational lifetime of an underlying structural surface of the weapon system. Polyurethane-based coatings are used universally in the defense, aviation, automotive, and medical industries because of their high impact strength at low temperatures and relative resistance to abrasion and degradation (Szycher, 2013). Ultimately, the degradation of these polyurethane coatings require a complex exchange between environmental (temperature, humidity, particulate, electromagnetic radiation exposure) and biological (biofilms, exopolysaccharides (EPS) composition, changes in local acidity) factors (Shah et al., 2008). The hydrolysis of these polymer coatings also liberates aliphatic and aromatic diols or carboxylates (in addition to intact polyurethanes blocks) into the environment. These foreign chemical species are of significant concern considering the increased use of polyurethanes in everyday life (Krueger et al., 2015), the dangers of microplastics in the environment (Paço et al., 2017), and also long-term health issues for aircraft personnel that work with or around areas where there is active biodegradation.

Several environmental testing protocols are available to evaluate the durability of a coating based on thermal-degradative, photo-degradative, and physical degradation mechanisms (Bierwagen and Tallman, 2001; Kiegle-Bockler, 2008). However, the world is not a sterile environment and coatings are typically compromised more rapidly in the presence of microorganisms. Thus, understanding biodegradative mechanisms while accounting for the natural attrition of the coating remains an active area of fundamental research and development (Kumar Sen and Raut, 2015; Loredó-Treviño et al., 2012; Restrepo-Flórez et al., 2014; Shah et al., 2014; Varjani and Upasani, 2017).

Polyester polyurethanes are more susceptible to hydrolysis than polyether or polyamide polyurethanes (Darby and Kaplan, 1968; Mahajan and Gupta, 2015). Several prokaryotic and eukaryotic microorganisms can hydrolyze polyesters and polyester polyurethanes while only fungi are reported to have hydrolyzed the more stable carbamate (Zafar et al., 2013) or alkene (Da Luz et al., 2015; Kumar Sen and Raut, 2015; Restrepo-Flórez et al., 2014) functional groups. Certain fungi can colonize plastic surfaces without the presence of other overt carbon source (da Silva et al., 2017; Oberbeckmann et al., 2016) suggesting that fungi are capable of degrading certain synthetic plastics and metabolizing some of the by-products from the biodegradation of the underlying synthetic polymer and many of the coating materials protecting our weapon systems.

In this SEED program we describe the isolation and identification of two yeast species, *Fungus 1* and *Fungus 2*, and a preliminary comparison to two fungal mold strains (*Fungus 3* and *Fungus 4*) isolated from the inside of aircraft that are active polyester polyurethane degraders. Qualitative Impranil[®] clearing results identified all fungi as potential polyester degraders from the consortia of microorganisms isolated from the same area of the aircraft. All fungi metabolized biodegradable polyesters (polyethylene succinate (PES) and polyethylene adipate (PEA)) in addition to the polyester polyurethane, Irogran[®] (previously called Morthane, Huntsman Corporation) (Powers et al., 2008). However, the polyether polyurethanes topcoats have demonstrated resistance to degradation by *Fungus 1* and *Fungus 2*. Fungal activity and the potential mechanisms for the degradation of these polymers were analyzed with both spectroscopic and headspace gas analysis. This is the first report of active polyester hydrolysis by *Fungus 1* and *Fungus 2* and a description of their activity compared to other polymer degrading fungal strains.

Materials and Methods

Isolation and identification of all fungal strains

All fungal strains were isolated from in-service aircraft using dry sterile nylon swabs to sample an area of approximately 3 x 3 inches. Sterile scissors cut the tip of the swab from the support into 0.5 mL of sterile phosphate buffered saline (PBS). The tube was sealed and processed by serially diluting in sterile PBS then plated onto Tryptic Soy Agar (TSA), Potato dextrose agar (PDA), and Artificial Sea Water Agar (ASW), and grown for 1 week at 27°C. Colonies on the initial culturing plates were re-streaked onto their respective media plates to isolate individual microorganisms to homogeneity. Isolated microorganisms were also cultured on TSA plates containing Impranil[®] (Bayer Material Science) to assess their ability to degrade polyurethane (data not shown). Impranil[®]DLN was used as received. The confirmed and identified fungal isolates were stored at -80°C in a final concentration of 20% glycerol in TSB.

For the yeast strain identification, isolates were inoculated into Tryptic Soy Broth (TSB) and grown overnight at 27°C. Each culture was centrifuged to pellet the cellular material and DNA was extracted from the pellet using ZR Fungal/Bacterial DNA MicroPrep[™] Kit kit (Zymo Research) following the manufacturer's instructions. PCR products were purified using the QIAquick PCR purification kit (Qiagen) according to manufacturer's instructions. Concentrations of purified PCR products were determined on a NanoDrop 9000 (NanoDrop Technologies). Sanger sequencing reactions (forward and reverse for each sample) were then carried out by North Carolina State University (NCSU) Genomic Sciences Laboratory (GSL) (Raleigh, NC). Electropherograms were analyzed using Sequencher[®] v5.2.4.

Growth and preparation of *Fungus 1* and *Fungus 2* cells for biofilm and planktonic culture experiments.

The growth of each fungus started from frozen 20% glycerol stocks inoculated into 5 mL of Yeast Mold (YM) Media (BD 271120) in 15 mL Falcon® Tubes. Each culture was shaken at 25°C at 120 rpm at a 45° angle for 36 hours using an orbital shaker to obtain an optical density at 600nm (OD_{600nm}) of 0.8 ± 0.1. Samples from these cultures provided the cells used to streak Tryptic Soy Broth (TSB) media (BD 211825) 1.5% (w/w) agar slants. Slants were incubated for 48 hours at 25°C. The working slant containing each fungus was then stored at 4°C for a period no longer than one month in duration. Prior to all experiments, cells from the working slants were transferred to sterile TSB culture media (5 mL) in 15 mL borosilicate culture tubes and incubated for 36 hours at 25°C with shaking (120 rpm). Cells from the TSB cultures were washed three times via centrifugation (1350 rcf, 1 min to pellet the cells, 1mL sterile water (for irrigation) for each wash). Cell suspensions in sterile water (for irrigation) were normalized to an OD_{600nm} = 0.6 ± 0.1 before they were drop-cast onto polymer-coated surfaces or used to inoculated planktonic growth experiments (Section 2.4).

Growth of fungi on atypical carbon sources in defined growth medium

A Bioscreen C Automated Microbiology Growth Curve Analysis System (Growth Curves USA) generated the optical density data for determining the difference in the growth between *Fungus 1* and *Fungus 2* on carbon sources applicable to the potential carbon sources generated from the hydrolysis of aliphatic polyesters and polyester polyurethanes. An evaluation of the growth of both strains in a defined minimal media (M9) over 48 hours at 25°C was performed in 96-well micro titer plates designed for the Bioscreen C. The growth density of each fungi was compared at pH 5.5 and 7.5 using all of the carbon sources. Sterilized M9 (Sambrook and Russell, 2001) defined growth media (adjusted from 7.6 to 5.5 drop-wise using concentrated phosphoric acid) was used as the stock medium for these growth experiments. Sterile aqueous stock solutions (PES syringe filter, 0.2 µm) of glucose, 1,3-diaminopropane, 1,6-diaminohexane, sodium succinate, sodium adipate, ethylene glycol, glycerol, 1,4-butanediol, and 1,6-hexanediol were stored at 4°C. The concentration of each carbon sources was 10 mM in each growth experiment and in acellular negative growth control experiments. We started growth experiments by adding 10 µL of the washed cell suspensions from section 2.2 to 225 µL of the growth medium with and without carbon sources. The 96-well plates contained triplicate growth experiments with acellular controls performed in duplicate on the same plate. The growth density was measured at 600 nm and was collected every 30 minutes in between cycles of vigorous shaking (120 rpm at a 2.5 cm orbit) from within the Bioscreen C system at 25°C.

Headspace gas analysis from polymer degradation experiments

Polyethylene succinate (PES; 10,000 MW determined by GPC) and polyethylene adipate (PEA; 10,000 MW determined by GPC) were purchased from Sigma-Aldrich and used as received. Both PES and PEA were dissolved in dichloromethane to a density of 80 mg/mL at room temperature. Irogran® pellets (PS455-203; Huntsman LLC.) were dissolved in tetrahydrofuran (THF) to a density of 80mg/mL at room temperature over 40 minutes. We added 200 µL of each polymer solution to sterile 11 mm diameter crimp-top autosampler vials. The solvents were removed via evaporation at room temperature over 2 hours and the residual

polymer-coated vials were incubated at 55°C for an additional 12 hours. After cooling, the vials were sterilized using UV-c radiation within a biosafety cabinet for 30 minutes.

Water-washed fungal cell suspensions (30 μ L) with an $OD_{600nm} = 0.6 \pm 0.1$ were drop-cast into each polymer-containing vial or control vials without polymer. Aluminum PTFE/SIL/PTFE crimp closures (Thermo Fisher Scientific) were used to seal the vials. The amount of water present in the sealed vials created an environment with a relative humidity of approximately 100% in biological triplicate. Positive control vials for this experiment contained no polymer and 30 μ L of the cell suspension (Control: Glass). Negative control vials contained each polymer with 30 μ L of sterile water. All control experiments were performed in parallel with active polymer biodegradation experiments at 25°C. We collected the changes in the gas composition from the headspace of each vial once per vial at 0, 1, 2, 3, 7 days after the vials were sealed (Fig. S1).

A custom Varian gas chromatography system (Varian 450-GC) with a thermal conductivity detector with a variable injection depth autosampler generated the separation of gases from 100 μ L gas injections. Data from the separation of three gas standards with known carbon dioxide concentrations (balanced with air) were used to generate the calibration curve for the concentration of CO₂ in mole % from a 100 μ L injection. The separation of carbon dioxide from other gases (example: oxygen and nitrogen) in a single chromatography run (Fig. S1-2) was completed using a system of custom pneumatic valves (Custom Solutions Group LLC) in conjunction with two packed columns (6' x 1/16" Hayesep Q 80/100 mesh column and 8' x 1/16" Molecular Sieve 5A 60/80 mesh column). The temperature of the column oven was 100°C.

Microscopic Analysis of Coating Degradation

PES, PEA, and Irogran[®] (80mg, PS455-203) were spin-coated onto glass and ZnSe surfaces using a Laurell spin coating system (Laurell Technologies Corporation). The concentration of polymer solutions that resulted in the most uniform coatings were 300 mg/mL CHCl₃ for PES, 150 mg/mL CHCl₃ for PEA, and 60 mg/mL THF for Irogran[®]. We drop-cast 0.1-0.2 mL of each polymer solution onto the supporting surface and initiated the spin-coating of the solution at an acceleration of 300 rpm to a maximum rotation rate of 1200 rpm for 30 sec under a nitrogen covering gas. The PES and PEA coatings were melted at 55°C for 12 hours and then rapidly cooled (on ice) for 5 min to between 4-5°C. This resulted consistently in 5-7 μ m thick coatings for PES and 6-10 μ m thick coatings of PEA.

Irogran[®] coatings were spin-coated using the same spin-coating method as PEA and PES but were heated to 100°C for 5 hours, placed in a 50°C incubator for 12 hours, and then finally allowed to cool to room temperature over 2 hours. The thicknesses of Irogran[®] coatings were 1.75-2.5 μ m. The coating thickness ranges were calculated using confocal profilometry from three independent samples using a Keyence VK-X250 3D Laser Scanning Confocal Microscope. UV-c light exposure sterilized all coatings from within a biosafety cabinet after 30 minutes.

All coatings were exposed to either 1 μ L drops of sterile water (for irrigation) or 1.2 x 10⁷ CFU/mL fungal cell suspensions in the same stock sterile water. The drops evaporated over 1-2 hours in the biosafety cabinet and each coating was placed in sterile screw-top 50 mL

Falcon[®] tubes containing 100 μL of sterile water. Each tube was incubated at 25°C. The amount of water used in these sealed Falcon[®] tubes maintained a relative humidity of 100% and resulted in minimal and reproducible levels of condensed water on the coated surfaces throughout the experiment.

The images of degradation were collected daily using a phase contrast (Phase 1) light microscope with a 10x objective and CCD color camera over the same region of the coating for seven days. The images show the changes that occurred at the boundary where the original spot dried and unexposed regions of the polymer (Supporting Information). After 8 days, these same degradation experiments were imaged with light and confocal laser mapping in order to generate depth profiles using a Keyence VK-X250 3D Laser Scanning Confocal Microscope highlighting regions of coatings exposed and unexposed to the fungal cells. A 100 μm x 100 μm 5-point polynomial-shaped area at least 1 mm from the boundary of the cells was used to set the baseline depth range and thus the general height profile scale for each experiment. Computer rendered maps of a collection of 200 μm x 200 μm individual laser depth profiles images (using a 50x objective) comprised the complete depth profile maps with both optical and laser data superimposed on the same image. The change in the depth profile determined the degree of degradation of the same polymers but using different fungal strains.

IR microscopy measurements of the degradation of Irogran[®] coatings

Irogran[®] was spin-coated onto 25 mm diameter x 2mm thick ZnSe windows using the same spin-coating protocols described in Section 2.6. Transmission micro-FTIR measurements were made using a Thermo Fisher Continuum FTIR microscope with a liquid nitrogen cooled MCT detector with a 50 μm spot size. The preparation of the cells for these experiments was described in Section 2.3. Thus, a triple rinsed fungal cell suspensions (1 μL) were drop-cast onto Irogran[®] coatings. The water comprising the drop of the cell suspension evaporated over 2 hours. This produced \sim 1 mm diameter spots containing monolayer aggregates of cells. If multiple experiments were performed on one coating, then the experiments were drop-cast with a spacing of $>$ 4 mm. After a 7-day incubation period at 25°C and 100% RH, regions covered with cells and the adjacent polymer-coated regions without cells were analyzed using FTIR. Reference FTIR spectra of the cells and polymer were collected separately.

AFM-IR Methods

AFM-IR contact-mode imaging and spectral analysis were done in air using an Anasys Instruments nanoIR in an ATR configuration with 450 μm Sicona probes. The IR source was a pulsed, tunable optical parametric oscillator laser providing 10 ns pulses at a 1 kHz repetition rate with \sim 8 cm^{-1} spectral resolution. AFM-IR spectra were determined from (PP-O)/BG where PP is the maximum peak to peak in the deflection signal of the cantilever ring-down, O (“offset”) is the average deflection signal measured in the absence of IR laser illumination, and BG (“background”) is the laser power measured by a separate photodetector. Thus, this calculation resembles 1/transmittance (1/T) in conventional optical spectroscopy.

During AFM-IR spectral acquisition, contact resonance frequencies were also simultaneously recorded and used to verify that the sample was not softening from heating

during laser exposure. AFM-IR signal averaging encompassed 256 pulses at each spectral frequency. Spectra were acquired at a data spacing of 4 cm⁻¹ and then smoothed using a 4 point average. Chemical maps were acquired at a 0.02 Hz scan rate with 32 pulse signal averaging. Unless indicated otherwise, all spectral and mapping data were acquired with a 20 kHz bandpass filter centered at 89 kHz, generally corresponding to the first contact mode resonance (ν_0) for the probe used in this work. Deviation from this frequency was never more than ± 2 kHz for the probe in contact with either PI or PU.

Results and Discussion

Isolation and Identification of *Fungus 1* and *Fungus 2* from microbial consortia collected from aircraft

Many in-service military aircraft are heavily used far beyond the age they were originally intended for and can potentially harbor substantial communities of microorganisms. In order to determine which members of these communities may be responsible for causing biodeterioration, we cultivated, isolated and identified microorganisms from in-service aircraft, and then screened those organisms based on their ability to clear Impranil[®] colloids embedded in agar plates (Cosgrove et al., 2007). Two organisms capable of clearing Impranil[®] in agar plates were identified as *Tremellomyces* fungi within the *Basidiomycota* phylum, *Fungus 1* and *Fungus 2*, via 16S, 18S, DNA and ITS rDNA region sequencing and phylogenetic data (Liu et al., 2015).

Fungus 1 and *Fungus 2* are non-pathogenic encapsulated yeasts from the phylum *Basidiomycota*. The presence of *Tremellomyces* yeasts inside the aircraft is congruous with the wide array of habitats and source materials already associated with the distribution of members of this class (May et al., 2016). However, neither of these strains has been reported to degrade synthetic polyesters or polyester polyurethanes.

Polymers and Polymer Coating Procedures

The degradation of a synthetic polymer by a microorganism (**Figure 1**) can be either the result of an indirect aggressive response (Indirect Biodegradation) to an environmental condition (temperature, competition with other organisms, water availability) or the direct search for a nutrient source (Direct Biodegradation). Both of these mechanisms begin with the hydrolysis of the polymer into more biochemically available functionalities. There are no surface receptors for aliphatic polymeric materials and thus a fungus cannot sense if a viable nutrient source is available without breaking the polymer into smaller chemical functionalities like disaccharides, carbohydrates, esters, and carboxylic acid compounds. This hydrolysis can occur by chemical and biochemical mechanisms even if the hydrolysis products from the polymer are not nutrient sources for the organisms. After hydrolysis, the response of the fungi will either be a result of the direct metabolism of the polymer (Direct Biodegradation) since it has generated a viable carbon source for growth or an indirect response (Indirect Biodegradation) to these products in the form of waiting for exposure to an external nutrient that it can use for survival. This indirect

response can also be induced from cells that were in a dormant state previously (Dormancy → Indirect Biodegradation) because the coating or environmental conditions resulted in a shift to a dormant cellular state. Indirect biodegradation mechanisms result in coating degradation but only as a result of cellular activity to another carbon source. Thus, the coating is not actually involved in the process that resulted in its degradation.

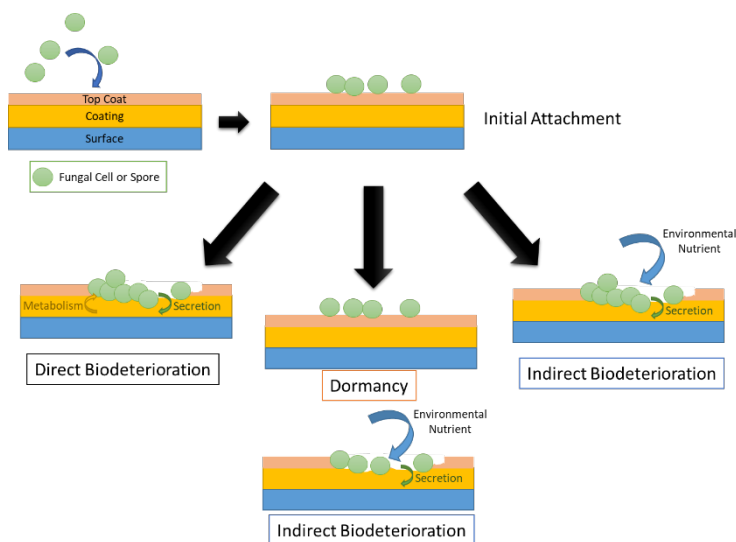


Figure 1 Schematic of the three outcomes resulting from the interaction of a microorganism with a synthetic polymer coatings.

If hydrolysis is inevitable, then how the microorganism responds to the liberated carbon source determines our ability to control degradation. In complex consortia, bacteria and fungi can create synergist relationships through an association called niche partitioning (Cortes-Tolalpa et al., 2017). This relationship can lead to the hydrolysis and metabolism of complex polymeric materials since the degradation of the polymer is delegated between two independent microorganisms. Our experiments show the biodegradation and metabolism of primarily aliphatic synthetic polymers using independent fungal strains though their role in the original environmental consortia is different from these isolated experiments. We have organized our program to approach degradation systematically using polymers with an increasing resistance to biodegradation based on composition. The general polymer progression is shown schematically in **Figure 2** and each arrow represents a go-no/go decision point since organisms that cannot hydrolyze polyesters and generate no oxidation products were not tested on polyether coatings. However, fungi that degraded polyesters were tested against the polyether polyurethanes.

Two polyesters and a polyester urethane, Irogran[®] were used to compare the differences in the degree of biodegradation generated by *Fungus 1* and *Fungus 2* biofilms (**Figure 3**). The two polyesters, polyethylene succinate (PES), and polyethylene adipate (PEA), are biodegradable by fungi and bacteria (Ishii et al., 2007; Kim and Rhee, 2003; Shah et al., 2014). The polyesters had identical molecular weights and were the polyethylene formulations so that both hydrolysis and the metabolites resulting from hydrolysis could be analyzed using the

biologically-relevant dioic acids, adipate and succinate. These dioic acids are key intermediates in amino acid or carbohydrate metabolism, respectively.

Irogran[®] is a well-defined thermoplastic aviation coating that is resistant to degradation by biofilms of *Pseudomonas fluorescens* Pf-5 (Biffinger et al., 2014). We chose Irogran[®] for these experiments since it has a published structure (Powers et al., 2008), defined formulation,

resistant to biodegradation, and the presence of adipate in the polyester segment of the polymer. Specifically, the hydrolysis of Irogran[®] would generate 1,4-butanediol, adipic acid, and potentially (though unlikely) 4,4'-methylenedianiline. The most probable hydrolysis by-product would be 4,4'-((methylenebis(4,1-phenylene))bis(azanediyl))bis(butan-1-ol) (**Figure 3**) instead of 4,4'-methylenedianiline based on hydrolysis of the ester instead of the carbamate linkage.

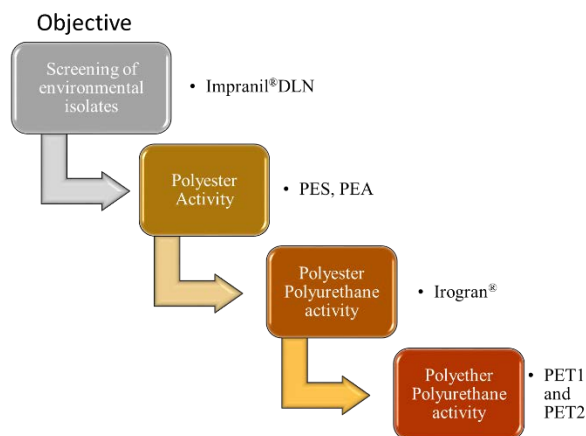


Figure 2 Organizational chart for increasing the polymer resistance to degradation based on coating composition

Biodegradation of polyethylene succinate and polyethylene adipate.

The clearing of Impranil[®]-containing agar plates by both *Fungus 1* and *Fungus 2* indicated that these fungi possessed esterase activity. Thus, we correlated the physiological and metabolic responses of each fungi during the degradation of PEA and PES coatings as biofilms. PES and PEA are biodegradable polymers and should result in the highest concentration of biologically-relevant nutrients from the coatings after hydrolysis as well as confirm that these fungi could degrade a polymer other than Impranil[®].

There are several approaches for calculating the metabolic responses from fungal cells. These include fluorescent metabolic stains coupled with microscopy, changes in transcriptional and translation profiles, and physiological changes based on morphology (Keller and Turner, 2013). We chose to analyze the activity of these fungi as biofilms on PEA and PES coatings with microscopy and through the production of CO₂ from the cells as a result of the metabolism of the coatings. The metabolism of both bacterial (Bester et al., 2010) and fungal systems can be calculated using CO₂ production (Stone et al., 2016b) and is a non-destructive method to assess the activity of these biofilms. We were interested in the general metabolic responses of each fungal strain during the biodegradation of each coating over 8 days. So, we analyzed the production of CO₂ with gas chromatography of the headspace of sealed gas chromatography vials at 25°C. The production of CO₂ from the degradation of PES and PEA by both *Fungus 1* and *Fungus 2* are shown in **Figure 4a and b**, respectively, over the first 7 days of the experiments. The baseline concentration of the CO₂ generated from the cells not exposed to any polymer but only the supporting glass surface are shown as black traces on each graph (Glass (Control) (**Figure 4**)).

The mass of each polymer and the number of water-washed fungal cells were standardized in each experiment to 16 ± 3 mg and 1.2×10^7 CFU/mL, respectively. By standardizing these variables, we were able to make comparisons between the activities of each fungal strain on the different polymers over time. The relative humidity (RH) for all experiments was approximately 100%. We chose an RH = 100% since these strains did not degrade Impranil[®] over 1 month if the RH was < 70% (data not shown). However, high humidity can limit the long-term survival of a fungus (Stone et al., 2016a) but for non-motile yeast the greatest rate of degradation occurred only at 100% thus far.

The baseline concentration of CO₂ generated from either fungus without the polymer present was 0.02 ± 0.01 mol% over 7 days **Figure 4**. *Fungus 1* produced the highest concentration of CO₂ (1.2 ± 0.2 mol %) from PES coatings **Figure 4a** while *Fungus 2* generated the highest concentration of CO₂ from PEA coatings **Figure 4b** over the same period. The concentration of CO₂ after 1 day was 1.5 times higher from *Fungus 1* on PES coatings than the concentration observed from *Fungus 2* on PEA coatings. This difference in CO₂ production between the strains became insignificant after 3 days of degradation. These data indicate that even though the highest concentration of CO₂ was generated from the degradation of these polyester coatings that the

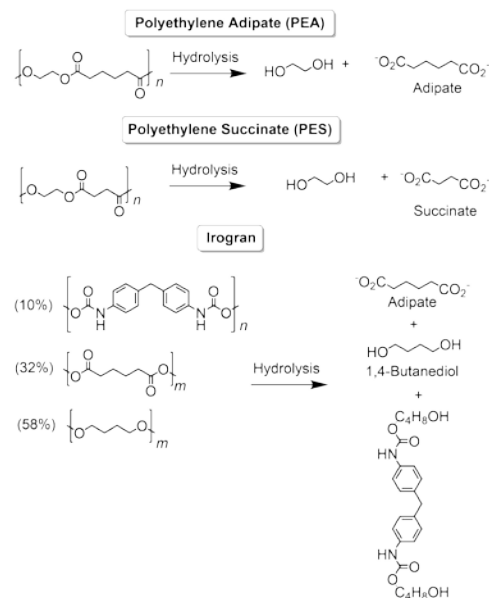


Figure 3 Chemical structures of Polyethylene Succinate (PES), Polyethylene adipate (PEA), and Imrogran[®] and the predicted hydrolysis products

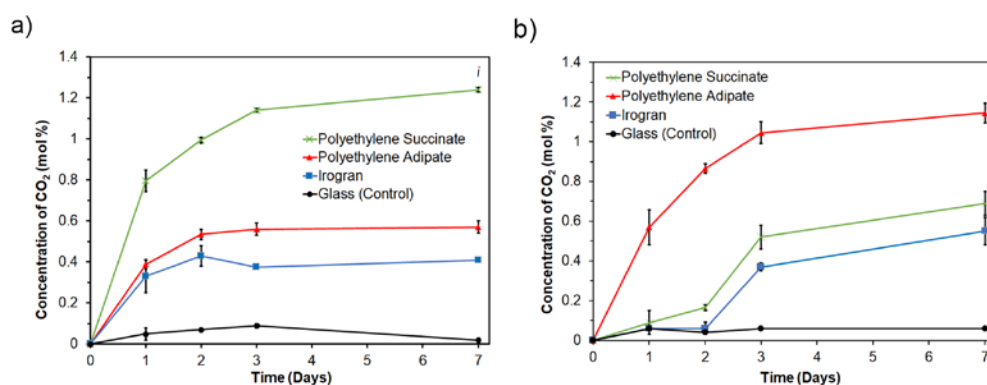


Figure 4 Time-dependent production of CO₂ by a) *Fungus 1* and b) *Fungus 2* from polyethylene succinate (PES), polyethylene adipate (PEA), Imrogran[®] and from vials without polymer with cells (Glass (Control)) during biodegradation over 7 days. ¹

¹ These data are a result of biological triplicate experiments starting from 30 μ L of water washed cell suspensions or just water (cell density: 1.2×10^7 CFU/mL). Relative humidity was 100% and vials were maintained at 25°C.

physiological differences could be significant between the same strain and the same coating material.

Since these experiments contained the same number of water-washed cells initially then the differences in total CO₂ production is a proxy for the response to degrading the polymer by each fungal strain. These data confirm that *Fungus 2*, compared to *Fungus 1*, was more active on adipate than succinate and that these strains of *Tremellomyces* oxidized both polymers to carbon dioxide as one of the main products. These differences in CO₂ production as a function of *Tremellomyces* strain and substrate also correlated well with the degree of qualitative clearing around colonies on Impranil®/agar plates (data not shown). The concentration of oxygen did not change significantly over 22 days confirming that the atmosphere was aerobic throughout the entire experiment. An example of the crude chromatogram from the headspace analysis after 22 days of degradation by *Fungus 1* on PES is shown in **Figure 5**. Maintaining an aerobic atmosphere in these sealed experiments is important for correlating the activity of these strains to the microscopy data using coatings open to the atmosphere over 8 days.

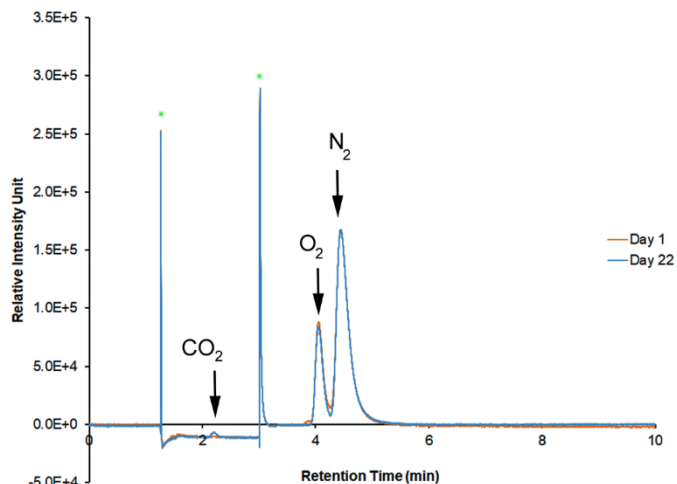


Figure 5 Representative average chromatographs from three biological replicates from gas sampled from the headspace over the active biodegradation of polyethylene succinate (PES) at 1 day (orange) and 22 days (blue) by *Fungus 1* at 25°C.²

These CO₂ results indicate that over a period of 7 days that each strain was actively degrading both PES and PEA to different degrees. In order to confirm this conclusion, we used phase contrast microscopy and confocal laser microscopy to compare the activity of each strain on the surface of PES and PEA coatings. We acquired images from the surface of each polymer over 7 days with phase contrast microscopy. These types of phase contrast images enabled non-destructive data to be collected from the same regions of the polymer over time. **Figure 6** and **Figure 8** show representative images from 0, 2, and 7 days after spotting *Fungus 1* and *Fungus 2* on the surface of PEA and PES, respectively. Each coating had same density of cells spotted on the surface at the beginning of the experiments. These images confirm that *Fungus 1* was spreading over the surface and changing the composition of the PEA and PES coatings over 7 days compared to *Fungus 2*. These images also show that PEA supported the growth of both fungi and that *Fungus 2* grew to a greater coverage and depth on PEA rather than PES coatings over 7 days.

² Green dots indicate the signal from pneumatic valve switching between packed chromatography columns.

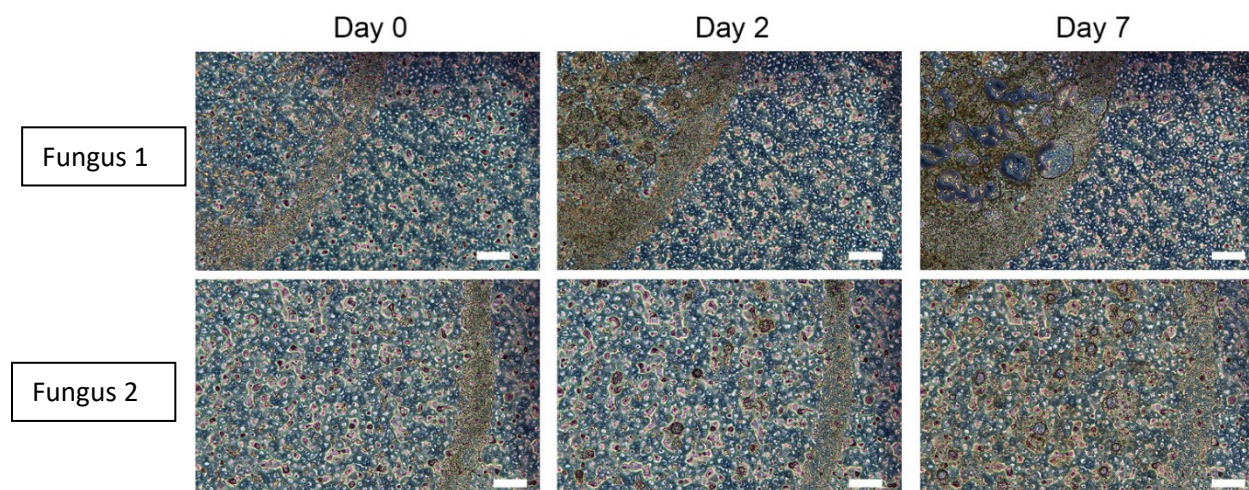


Figure 6 Selected time-dependent phase contrast (Phase I) optical microscopy images of a region of a PEA coating exposed to *Fungus 1* or *Fungus 2* after the initial exposure (Day 0) and 2 and 7 days after exposure.³

Confocal profilometry with overlapping optical images of both fungi on PES and PEA were collected on the 8th day of the experiment. The resulting rendered maps show the degradation of PEA by *Fungus 1* and *Fungus 2* (**Figure 7a** and **c**, respectively). Depth profiles were calculated along the lines rendered on **Figure 7a** and **c** and are shown in **Figure 7 b** and **d**, respectively. The color-coded lines in **Figure 7** represent the path and the fungal strain of the calculated changes in coating thickness across the original boundary of the cells onto the undegraded polymer region. The depth data collected from the control coatings (**Figure S1-Figure S3**) over the same period showed no sign of degradation and these data were plotted as grey lines on the depth profile charts in **Figure 7**. Our results confirm that the degradation of PEA required fungal cells and that significant degradation and loss of the coating occurred using both strains. The degree of degradation by *Fungus 1* coupled with its rapid growth shown in **Figure 6** and **Figure 7** confirms that *Fungus 1* degraded PEA to a greater degree than *Fungus 2*.

³ Scale bars are 100 μm . Experiments were maintained under identical environmental conditions (100% RH, 25°C) with control experiments (exposed to sterile water instead of cell suspensions) showing no signs of degradation.

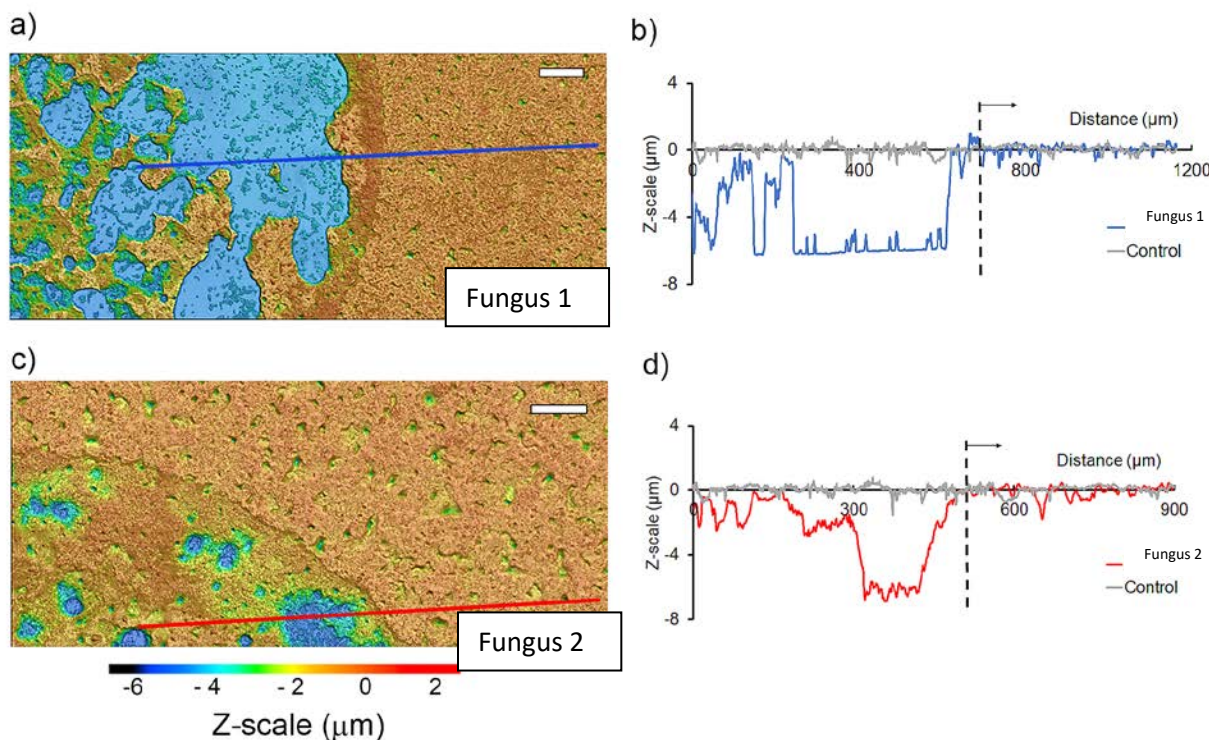


Figure 7 Overlapping scanning confocal laser profile and optical images of PEA coatings exposed for 8 days to a) *Fungus 1* , c) *Fungus 2* . The lines rendered onto images a and c indicate where 2-point height profiles were extracted for b) *Fungus 1* (blue line), c) *Fungus 2* (red line) compared to sterile water (control) (grey line; from **Figure S1**.⁴

In the case of *Fungus 1* , rapid growth coupled with its lack of mobility led to cells that are no longer in contact with the polymer. This could be an explanation for why the production of CO₂ was so high on day 1 compared to *Fungus 2* on the same day since both CO₂ rates decreased rapidly over the 7 days (**Figure 4a**). This was in spite of the more aggressive degradation of *Fungus 1* compared to *Fungus 2* . Even though the biodegradation of PEA was significant within the boundary of the original *Fungus 1* cell suspension drop (appears as an elevated ring of cells on **Figure 7a-b**), the degradation of the polymer appeared to stop at this boundary and suggests that the degradation of this polymer was based on the free diffusion of secreted hydrolytic enzymes from *Fungus 1* cells not at the boundary. The degradation mechanism of *Fungus 2* is not as obvious and the general decrease in height around the boundary of the original cell spot (**Figure 7c-d**) does indicate these two fungi use different mechanisms during the degradation of PEA.

⁴ Experiments had a RH= 100% at 25°C. White scale bars define X and Y distances on the images and are 100 μm.

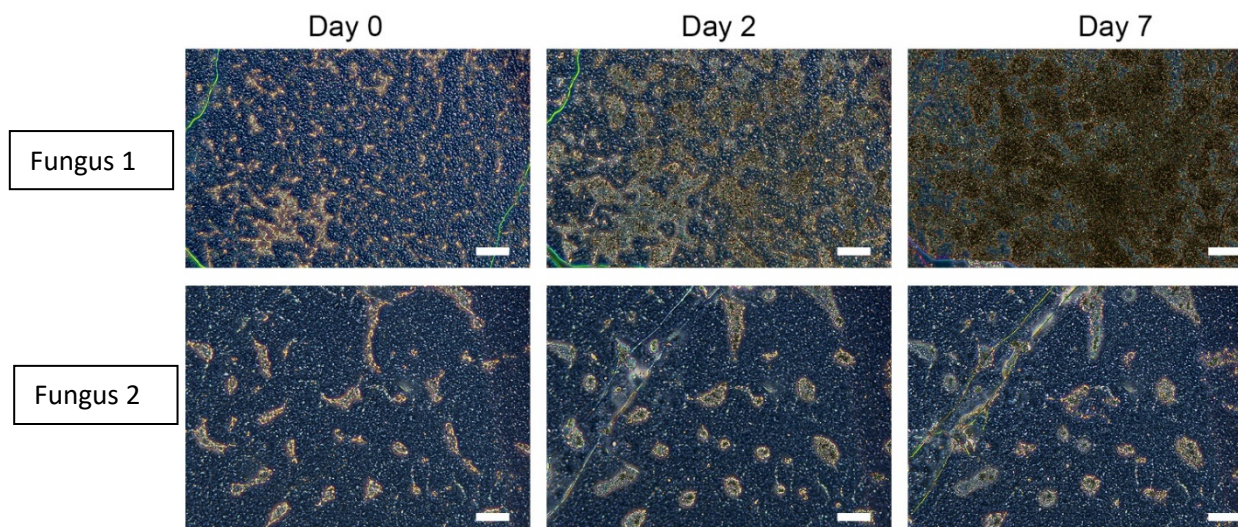


Figure 8 Selected time-dependent phase contrast (Phase I) optical microscopy images of a region of a PES coating exposed to *Fungus 1* or *Fungus 2* after the initial exposure (Day 0) and 2 and 7 days after exposure.⁵

Fungus 1 and *Fungus 2* degraded PES coatings differently than the PEA coatings. Phase contrast microscopy images after the cell suspension dried (day 0) and then 2, and 7 days later show that *Fungus 1* grows on the surface of PES coatings (**Figure 8**). *Fungus 1* grew over the PES surface within the boundary of the original cell spot similar to what occurred on PEA coatings, while *Fungus 2* did not grow well on the PES surface except within cracks that formed naturally using these coatings (**Figure 8**). There were only slight changes in the shapes of the *Fungus 2* cell masses over time. In general, PES coatings cracked to the same degree with or without fungi on the surface. These cracks did lead to expansive fungal growth compared to cell masses on the uncracked areas, but the cracks were not a direct result of the degradation of the PES coating.

⁵ Scale bars are 100 μm . The fractures observed in these coatings were also observed in control coatings that were not exposed to cells but maintained under identical environmental conditions (100% RH, 25°C)

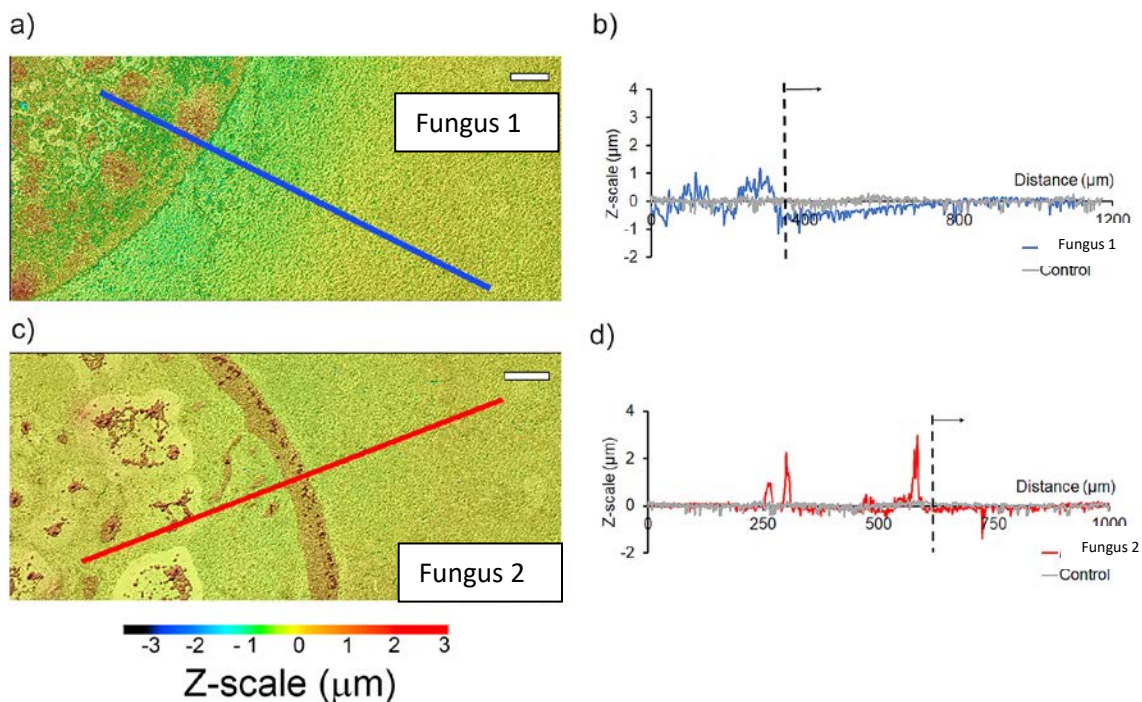


Figure 9 Overlapping scanning confocal laser profile and optical images of PES coatings exposed for 8 days to a) *Fungus 1*, c) *Fungus 2*. The lines rendered onto images a and c indicate where 2-point height profiles were extracted for b) *Fungus 1* (blue line), c) *Fungus 2* (red line) compared to sterile water (control) (grey line; from **Figure S2**).⁶

On the 8th day, confocal profilometry images were collected and generated the resulting compiled maps showing the degradation of PES by *Fungus 1* and *Fungus 2* (**Figure 9a** and **c**, respectively). Depth profiles were calculated along the lines rendered on **Figure 9a** and **c** and are shown in **Figure 9b** and **d**, respectively. The grey traces show the depth profile calculated from a control PES coating exposed to sterile water instead of the water/cell suspension over the same period (**Figure S2**). The degradation of PES coatings by *Fungus 1* was significantly less than the degradation of PEA coatings at the beginning of the experiment and over the first 8 days. Based on the confocal profilometry results, *Fungus 2* did not generate any significant changes in the thickness of the coating while *Fungus 1* produced a 300 μm radius of coating loss extending from the edge of the original boundary of the cell suspension drop (**Figure 9a**). The largest change in the depth of the PES coating (> 1 μm) was within the boundary of the cells and thickness of the coating gradually increased over a distance of 400 μm from this boundary (**Figure 9b**). This degradation pattern indicates that the cells were secreting hydrolases at some point and that these active hydrolases stopped being secreted and were no longer active based on how far they diffused from the fungal cell masses. There was no loss of coating near the boundary of *Fungus 2* cells nor within the original cell spot (**Figure 9c+d**) area.

⁶ Experiments had a RH= 100% at 25°C. White scale bars define X and Y distances on the images and are 100 μm.

These degradation images are consistent with the CO₂ production results (**Figure 4**) since *Fungus 1* grows on the surface of PES resulting in high concentrations of CO₂ while *Fungus 2* produced 50% less CO₂ and did not grow on the surface of PES. The combination of these results suggests that *Fungus 1* can utilize succinate or is less sensitive to ethylene glycol than *Fungus 2* since degradation occurred earlier in the experiment. Some of the *Fungus 2* cell mass appeared to smooth the coating but did not remove the coating (**Figure 9c**). There was no smoothing of the coating surface around the cells that made up the boundary of the original cell spot which also indicates that these cells were not active over the entire 8 days.

The Biodegradation of Irogran[®] using non-motile yeast strains: A Polyester Polyurethane Coatings

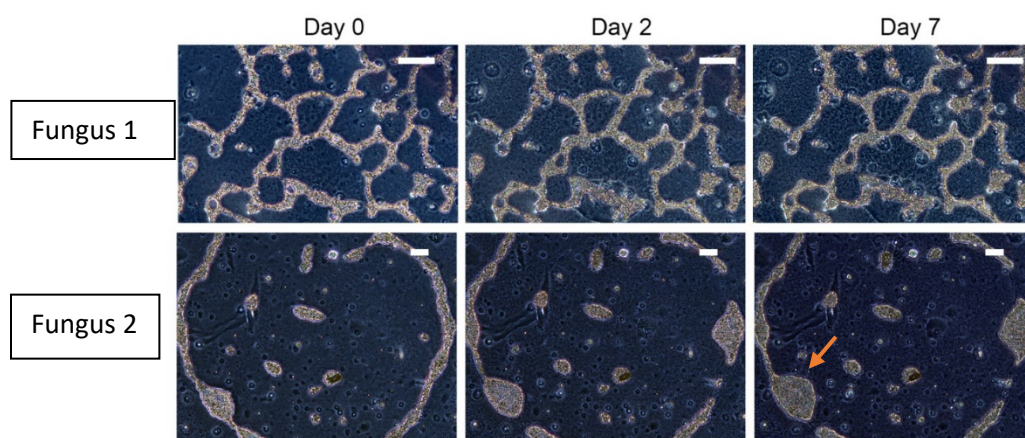


Figure 10 Selected time-dependent phase contrast (Phase I) optical microscopy images of a region of a Irogran[®] coating exposed to *Fungus 1* or *Fungus 2* after the initial exposure (Day 0) and 2 and 7 days after exposure.⁷ The orange arrow shows the same cell mass as indicated in **Figure 12**.

To date, Irogran[®] has resisted degradation by one bacterial strain, *P. fluorescens* Pf-5 (Biffinger et al., 2014). The aggressive degradation of PES and PEA coatings by *Fungus 1* indicated that *Fungus 1* might be able to degrade Irogran[®] based on its composition. We first collected time dependent phase contrast microscopy images of the same region of the Irogran[®] surface exposed to *Fungus 1* and *Fungus 2* (**Figure 10**). Briefly, over the duration of the experiment the *Fungus 2* cells collected gradually into larger masses which were observed by the gradual thinning of cells directly adjacent to increasing cell masses. One such area is highlighted with an orange arrow on day 7 (**Figure 10**). *Fungus 1* cells did not change their location as obviously as *Fungus 2* over the duration of the experiment. We also did not observe

⁷ Scale bars are 100 μ m. Experiments were maintained under identical environmental conditions (100% RH, 25°C) with control experiments (exposed to sterile water instead of cell suspensions) showing no signs of degradation.

the same degree of cellular growth on Irogran[®] coatings as we did on PES and PEA coatings (Data not shown).

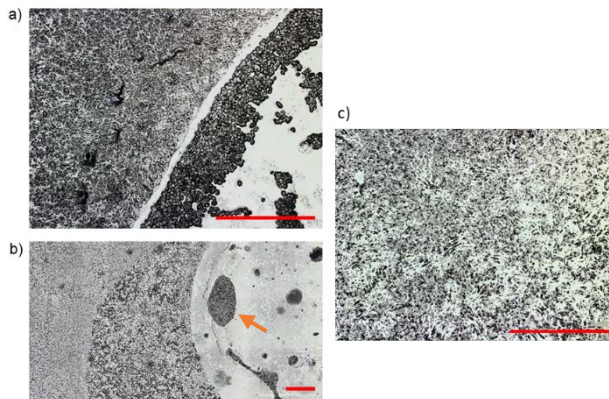


Figure 11 Overlaid scanning confocal laser profile and optical images of Irogran[®] coatings exposed for 8 days to water-washed suspensions of a) *Fungus 1* , b) *Fungus 2* , or c) sterile water at RH: 100% at 25°C. Images were taken at the boundary of the drop of the original sample. Red scale bars set to 100 μm . The orange arrow shows the same cell mass as indicated in **Figure 10**.

In addition to the phase contrast microscopy images over 7 days, confocal profilometry images after 8 days showed a general smoothing of the polymer surface from within the boundary of the original spot of cells for both *Fungus 1* (**Figure 11a**) and *Fungus 2* (**Figure 11b**). These images were collected to highlight boundary of the original spot. The region that was exposed to the original spot was smoother than anywhere else around this area. This change in surface texture was due to the fungi since the surface texture of control Irogran[®] coatings (exposed to a 1 μL water drop) did not result in a smoothing of the coating over the same time period (**Figure 11c**). This smoothing of the polymer was uniform around the entire spot and indicates that when the *Fungus 2* cells were first spotted that they were degrading the polymer, but over time became deactivated or were dormant, as they pooled since the degree of degradation did not increase as the cells amassed into specific areas. Interestingly, *Fungus 2* also generated areas of smooth polymer but did not degrade PES coatings. Thus, at the early stages of the degradation process both cell types changed the polymer surface but over time *Fungus 1* actually degraded Irogran[®].

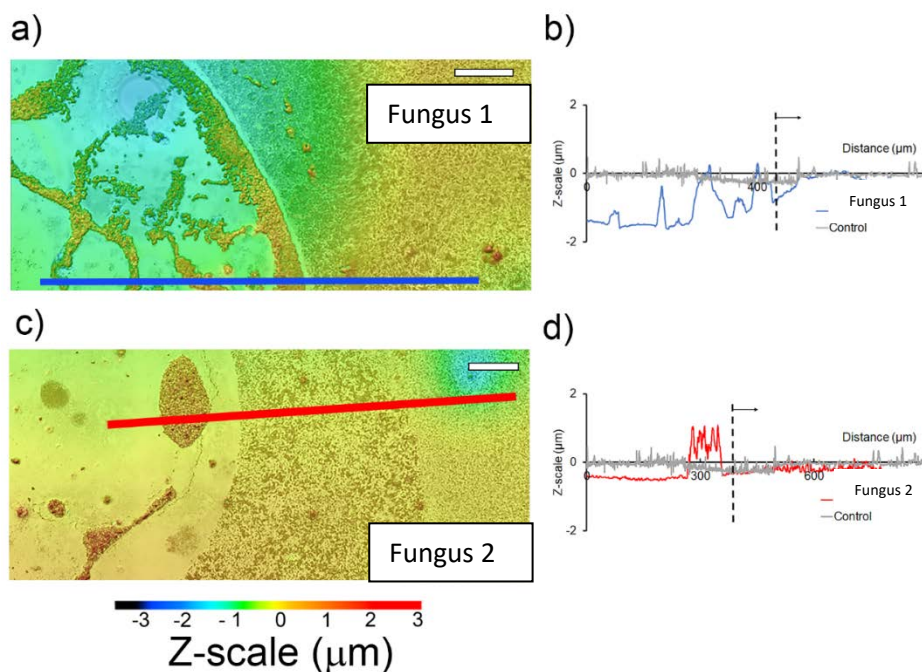


Figure 12 Overlaid scanning confocal laser height profile and optical images of Irogran[®] coatings exposed for 8 days to a) *Fungus 1* and the b) resulting height profile from the rendered blue line on (a), c) *Fungus 2*, and the d) resulting height profile from the rendered red line on (c). Grey height profiles on (b) and (d) were calculated from sterile water results (control; **Figure S3**).⁸

Both fungi also produced carbon dioxide after exposure to Irogran[®] over 8 days at a RH: 100% (**Figure 4**) suggesting that degradation was occurring. The maximum concentration of CO₂ produced from either fungus from Irogran[®] was between 0.5-0.6 mol% after 8 days. This was approximately half of the concentration of CO₂ generated from PES coatings by *Fungus 1* or PEA coatings from *Fungus 2*. The amount of CO₂ produced by *Fungus 2* on Irogran[®] coatings followed a similar trend to the CO₂ produced from PES coatings which were not degraded readily by *Fungus 2*. The opposite is true for *Fungus 1* which showed the same magnitude and trend of CO₂ production as what occurred during the degradation of PEA coatings.

The degradation of Irogran[®] was also analyzed using changes in the depth of the coating around cell masses which would be an indicator of degradation. However, this data also resulted in our first evidence of the role of water in the degradation process using the non-motile yeasts. Experiments performed at a relative humidity of 100% include the gradual condensation of water over the entire surface. We optimized our experimental protocol does eliminate large pools of water forming on the surface but rather induce a uniform coverage of water over the surface. Our Irogran[®] coatings also contained 100 µm diameter and 1 µm deep circular imperfections (**Figure S3**). On control coatings, these imperfections did not change size (**Figure S3**) nor depth (grey

⁸ Experiments were maintained at RH 100% at 25°C. White scale bars define X and Y distances on the images and are 100 µm.

traces in **Figure 12b** and **d**) over the 8 days.

Figure 12a shows that the most significant loss of the Irogran[®] coating using *Fungus 1* occurred in a region that was not necessarily where the bulk of the cells was located. If the cells were actively degrading the surface, then we would expect degradation patterns originating from areas with the greatest cell density. Instead, these images suggest that over the 8 days that the activity was pooled into areas that were initially lower than the rest of the sample. We were able to see this effect since the general rate of Irogran[®] degradation was slower than what we observed with *Fungus 1* on PEA and PES coatings. Some of the Irogran[®] coating was removed by *Fungus 2*, albeit about 2-fold less than *Fungus 1*, based on the difference in the depth profiles shown in **Figure 12 b** and **d**.

Infrared spectroscopy data of the degradation of Irogran[®]

Some of the most chemically significant data for the biodegradation of polymer coatings has been acquired using IR spectroscopy (Biffinger et al., 2014; Christenson et al., 2007; Mahajan and Gupta, 2015). In this work, transmission infrared (IR) microscopy was used to spectroscopically detect and analyze chemical degradation of Irogran[®] underneath *Fungus 2* or *Fungus 1* cell masses. The general approach was to first collect transmission μ IR spectra of a biofilm – polymer bilayer region and an adjacent region of the polymer film without the biofilm (within ~ 500 μ m). Difference spectra were then generated by subtracting the “polymer only” spectrum from the “biofilm on polymer” spectrum allowing biofilm induced changes to the polymer to be distinguished. In these samples, interference of the biofilm was low enough so that changes occurring to the polymer could be readily identified.

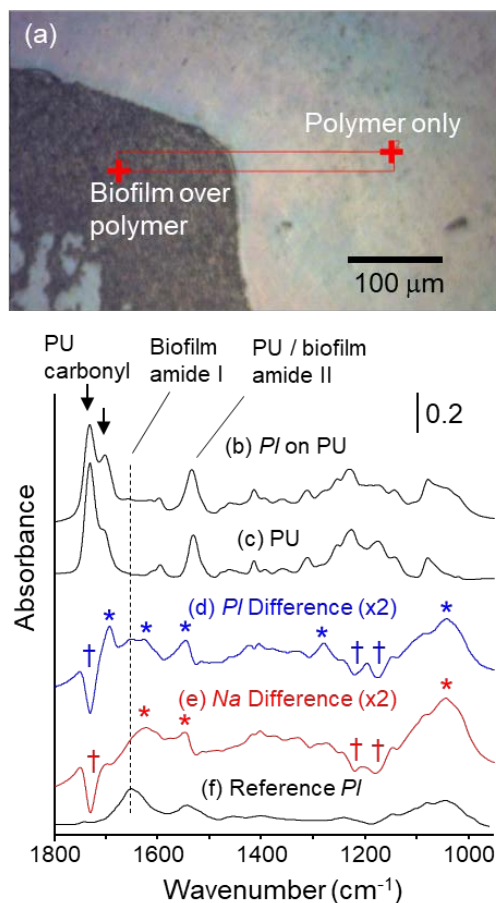


Figure 13 Infrared microscopy data from the biodegradation of Irogran[®] coatings (PU) on ZnSe windows using drop cast *Fungus 1* (PI) at 100% humidity (25°C). a) Optical image of *Fungus 1* drop-cast on Irogran[®] coating with spectra collected at the ‘+’ marks (b,c) Spectra collected on and off the biofilm, respectively. Vertical arrows identify the 1735 cm^{-1} and 1700 cm^{-1} carbonyl peak and shoulder. (d) Difference spectrum for ‘b’ – ‘c’. Asterisks and daggers identify positive and negative peaks. (e) Difference spectrum collected by same procedure for *Fungus 2* on Irogran (f) Spectrum of *Fungus 1* biofilm on ZnSe with no polymer layer

Results are shown in **Figure 13**. **Figure 13a** shows a representative optical image at the edge of a monolayer cluster of *Fungus 1* cells (dark grey mass on the left half of the image) on the Irogran® coated ZnSe window prepared for FTIR microscopy. **Figure 13b,c** shows spectra acquired on and off the cells, respectively, and **Figure 13d** shows the corresponding difference spectrum. **Figure 13e** shows a difference spectrum obtained using the same method for a *Fungus 2* biofilm on Irogran and **Figure 13f** shows a biofilm spectrum of *Fungus 1* cells deposited on ZnSe (without polymer coating).

Notable polyurethane spectral features in **Figure 13** include the peak and shoulder at 1735 and 1700 cm^{-1} identified with vertical arrows. These are attributed to non-H bonded and H-bonded carbonyls, respectively, for the ester and urethane components (Chen et al., 2001). The urethane amide II peak appears at 1535 cm^{-1} and an amide II peak for the biofilm also appears at 1544 cm^{-1} . The biofilm also has an amide I peak near 1650 cm^{-1} . Comparison of the “PU” and

“Reference *PI*” spectra (**Figure 13 c,f**) show that there is little interference of the biofilm in the PU carbonyl region and that there is

also little interference of polymer peaks in the biofilm amide I region. In contrast, the PU and biofilm amide II peaks are in partially overlapping regions. However, the “*PI* on PU” spectrum (**Figure 13b**) shows that the biofilm amide I peak is not

Table 1 Differential peak positions from **Figure 13d,e**

PI ⁺ peaks (cm^{-1})	Na ⁺ peaks (cm^{-1})	PI ⁻ peaks (cm^{-1})	Na ⁻ peaks (cm^{-1})	assignments
		1732	1732	Ester carbonyl loss
1696				H-bonded carbonyl; conjugated C=O
1628	1628			Carboxylate degradation product?
1547	1547			Carboxylate degradation product
1279				v(C-O), conjugated ketone degradation product
		1220, 1181	1220, 1181	Ester C-O loss
1045	1045			v(C-O) Alcohol degradation product

prominent relative to the neighboring polymer peaks. This shows that interference of biofilm features will be minimal for distinguishing polymer changes in the difference spectra.

The difference spectra in **Figure 13 d,e** show both positive and negative peaks that can be attributed to polymer changes caused by the biofilm. Positive peaks, marked with asterisks, identify new chemical features that have appeared, and negative peaks, marked with daggers, indicate chemical features that have been lost from the polymer. These positive and negative peaks are tabulated in **Table 1**. The difference spectra (**Figure 13d,e**) show negative peaks near 1735, 1220, and 1181 cm^{-1} , indicating loss of carbonyl and C-O functionalities. These are attributed to loss of the ester component from the polymer. A positive peak also appears for both difference spectra at 1547 cm^{-1} which has previously been correlated with a carboxylate degradation product from polyester hydrolysis (Biffinger et al., 2014). The difference spectra also show peaks near 1045 cm^{-1} corresponding to diol degradation products. (The absorption intensity in this region is above that expected for the relative intensity of the biofilm alone.)

Carbonyl loss could also be due to degradation of the urethane component, although no obvious negative peaks are observable for the urethane amide II at 1535 cm^{-1} . However, this region is also partially impacted by the biofilm amide II and the carboxylate degradation product signature. To better ascertain if any urethane or polyether degradation was occurring, the same type of measurement was also done for a *Fungus 1* biofilm on an PET1 polyether polyurethane coating. **Figure 14** shows the resulting spectra for the biofilm on PU, PU only, and the difference spectrum. The difference spectrum reproduces the biofilm spectrum and shows no detectable loss of the urethane or ether components. This confirms the primary mode of Irogran[®] degradation as ester hydrolysis, most likely through lipase activity.

Additional peaks in the **Figure 13** difference spectra are less straightforward to identify. The peak at 1628 cm^{-1} could also be a carboxylate related degradation product. The *Fungus 1* difference spectrum also shows peaks at 1696 and 1279 cm^{-1} not apparent in the *N. albidus* spectrum. The 1696 cm^{-1} peak could be due to an increase in H-bonded carbonyl due to rearrangement of the remaining polymer components, although it's not clear why this wouldn't happen for *Fungus 2* as well. The additional peaks may also be representative of varying chemical environments due to inhomogeneous degradation and / or further metabolization of adipate and the diol metabolites. Otherwise, both sets of live cells show similar intensity negative losses at 1735 cm^{-1} indicating similar levels of Irogran[®] degradation, although the cells may not metabolize the degradation products to the same extent. Collectively, these data confirm that *Fungus 2* and *Fungus 1* actively degraded Irogran[®] at 100% RH and hydrolyzed the soft polyester segment of the polymer in preference to the hard polyurethane segment, consistent with lipase activity.

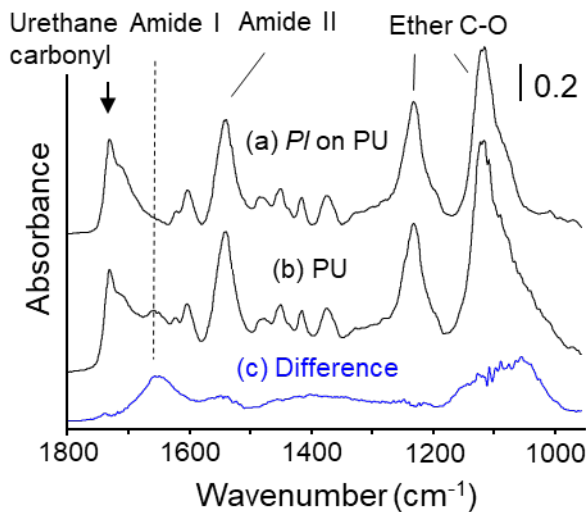


Figure 14 Transmission micro FTIR spectra of (a) *Fungus 1* on PET1 polyether polyurethane film (b) adjacent biofilm free region of the polymer (c) difference spectrum

Confocal Raman Microscopy Depth Analysis from the Degradation of Irogran[®] using *Fungus 1*.

In addition to FTIR, the viability of confocal Raman microscopy was investigated to map degradation and bulk polymer loss in $\sim 10\text{ }\mu\text{m}$ thick Irogran films. One advantage with this method is that the trenches can be non-destructively, three-dimensionally mapped underneath the cells. Thus, the true trench dimensions can be determined without interference from the overlying cells and ultimately the movement of water can be mapped throughout the coating if the humidity of the sample can match the humidity of the chamber. An additional advantage is

the Raman mapping yields chemical information that provides insights into the degradation mechanisms. Our data for *Fungus 1* shows (Figure 15) demonstrating a similar trench formation on Irogran, although progressing at a much slower rate than on Impranil®. In the top figure we are mapping the location of the biofilm after 15 days and the lower figure shows the location of the polyester component. The PU carbonyl map shows loss of the ester component in the region underneath the cells as also was indicated by FTIR.

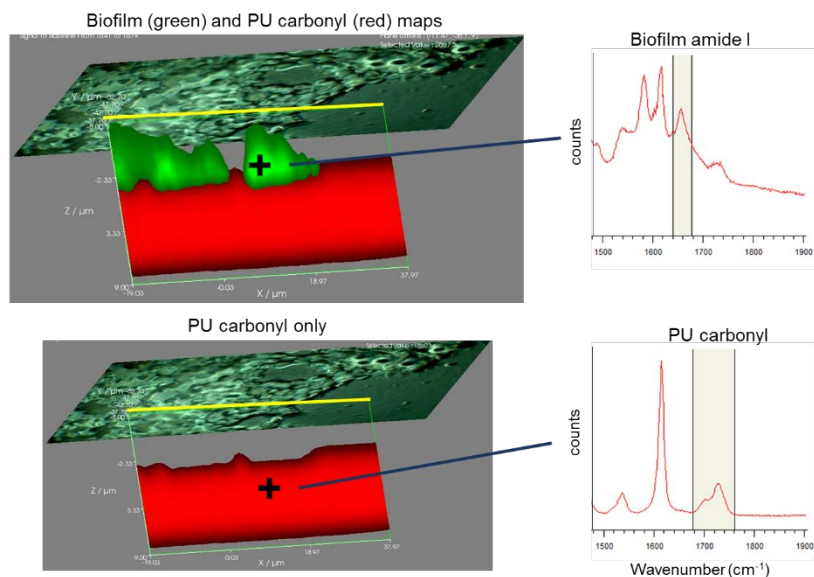


Figure 15 Raman depth slices acquired from a *Fungus 1* biofilm on a ~ 10 µm Irogran® film. The upper left figure shows an optical image at the top and depth slice data below. The optical image is viewing the underside of the biofilm through the polymer and the yellow line indicates the location the depth slice was acquired.⁹

Comparing of the planktonic growth of all fungal strains on carbon sources generated from polymer hydrolysis to the growth observed on PES, PEA, and Irogran®.

The results we have presented thus far confirm that *Fungus 1* grew and degraded PES and PEA coatings within the area of the original location of cells over the first 8 days of exposure. *Fungus 2* grew best on PEA rather than PES coatings. However, was this metabolism and degradation activity due to the liberation of the hydrolysis products? Thus, we compared the growth density of *Fungus 1* and *Fungus 2* as planktonic cultures after 48 hours using an array of aliphatic diols and dicarboxylates as the sole carbon sources at pH 5.5 and 7.5 (Figure 16). Glucose was used as a positive control for growth since a majority of species in the *Tremellomycetes* genera are commonly found on or near decaying biomass or fecal waste and possess hyaluronan (Smirnou et al., 2015) and xylan hydrolysis activities (Lara et al., 2014).

⁹ Green corresponds to the biofilm amide I intensity and red corresponds to the PU carbonyl intensity. The lower left figure is the same as above except only the PU carbonyl map is shown. Selected spectra are shown to the right identifying the peaks used to generate the color maps. The PU carbonyl depth slice shows shallow trenches forming in the biofilm covered region.

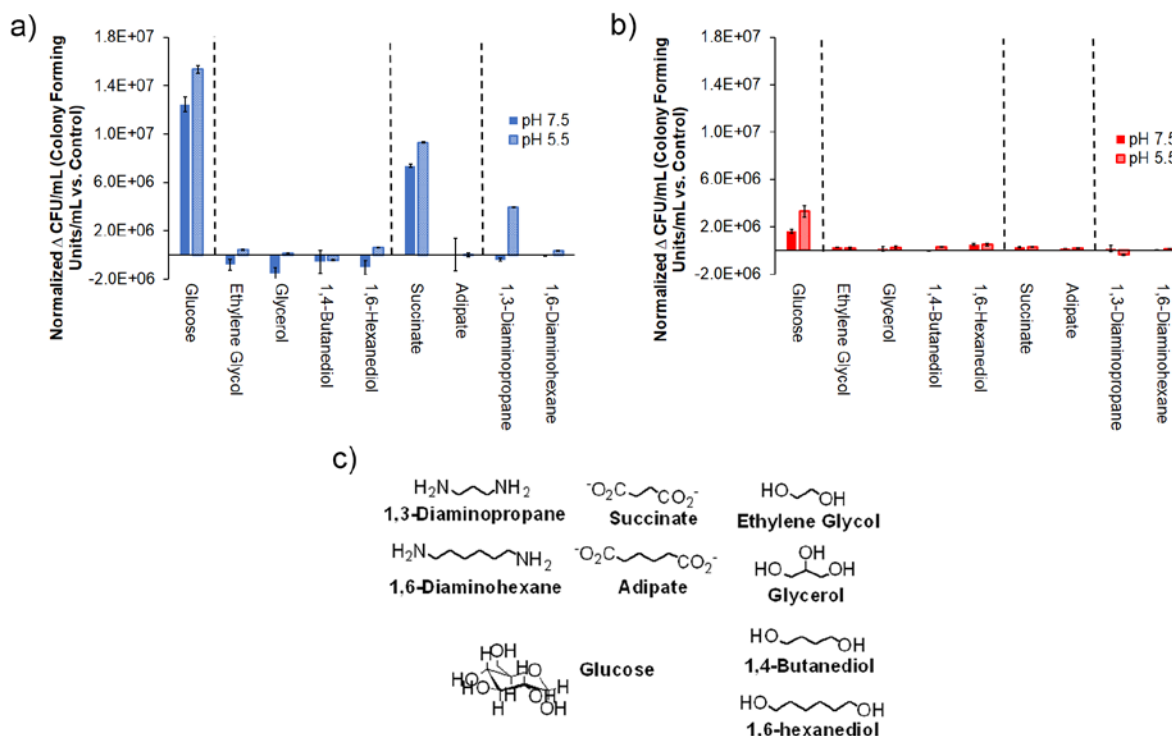


Figure 16 Normalized cell densities of 48 hours planktonic cultures of a) *Fungus 1* and b) *Fungus 2* in M9 media at either pH 7.5 or 5.5 with carbon sources potentially generated from the hydrolysis of PES, PEA, and Irogran[®] coatings or similar aliphatic polyester polyurethane coatings, and (c) Structure and naming of the carbon sources used for growth.¹⁰

We confirmed that none of these carbon sources were toxic to the cells at a 10 mM concentration from differences in the cell densities of each fungi in 1:10 TSB/water media supplemented with each carbon source at 10 mM (**Figure S4**) after 48 hours to their growth in 1:10 TSB only. Our results confirm that none of these carbon sources (and more importantly the diols liberated from the hydrolysis of all of the polymer coatings (ethylene glycol or 1,4-butanediol)) were acutely toxic to these actively growing fungi.

Based on this toxicity screen we used a minimal nutrient growth medium (M9) (Sambrook and Russell, 2001) with these carbon sources adjusted to either pH 5.5 or 7.5 for the actual growth comparisons since growth data generated from a diluted nutrient rich medium would not be represent of the conditions these cells experienced on the polymer surface. These two acidities were chosen based on potential local pH changes that can occur during the

¹⁰ The concentration of carbon sources were 10 mM. Graphs were calculated using the density of cells in colony forming units/mL (CFU/mL) at 25°C normalized to control experiments inoculated with cells but did not contain a carbon source. All experiments were performed in biological triplicates.

hydrolysis of a polyester. Optical densities were measured at 600 nm. These data were then standardized to actual cell counts/mL using cytometry so that the density of cells inoculated into the growth experiments was identical.

The results shown in **Figure 16** show two very different responses to these carbon sources and growth conditions. *Fungus 1* grows to 8 times the cellular density over 48 hours than *Fungus 2* on glucose and both strains grow to 20% higher density at pH 5.5 compared to pH 7.5. The fact that both strains grow to higher densities at higher acidity is consistent with the acidic conditions used to culture each fungal cell type from the frozen stock or commercial lyophilized materials (pH = 4.5). This inherent tolerance to acidic conditions is an advantage for these fungi since the degradation of a polyester will shift the local pH to higher acidity over time. Regardless, these results with glucose confirm that the media formulation does support the growth of each fungi as planktonic cultures.

A comparison of the planktonic growth results using the rest of the carbon sources resulted in nowhere near the density of cells grown with glucose. One common difference between *Fungus 1* and *Fungus 2* was the generally higher cell densities produced by *Fungus 1* compared to *Fungus 2* after 48 hours. This difference in the planktonic growth density was mirrored in each organism's growth on PEA coatings, with *Fungus 2* growing and degrading PEA but to a significantly lesser degree than *Fungus 1* (**Figure 6**). With regards to individual carbon sources, *Fungus 1* grew using succinate at both pH 7.5 and 5.5 and with 1,6-hexanediol and 1,3-diaminopropane at pH 5.5 (**Figure 16a**). *Fungus 2* did not produce measurable planktonic growth using any of these carbon sources with exception to 1,6-hexandiol and 1,4-butanediol at pH 5.5 (**Figure 16b**).

Fungi	Glucose	1,3-diamino propane	1,6-diaminohexane	sodium succinate	sodium adipate	ethylene glycol	glycerol	1,4-butane diol	1,6-hexane diol
<i>Fungus 1</i>	x	x (pH 5.5 only)		x					
<i>Fungus 2</i>	x							x	x
<i>Fungus 3</i>	x						x	x	
<i>Fungus 4</i>	x			x					

x designates that change in optical density (at 600nm) of the culture was > 0.05 after 48 hours of growth at 25°C. Carbon sources were used a concentration of 10 mM.

A summary of our growth results using all of the fungal strains proposed in the SEED program are presented below in **Table 2**. The growth conditions for fungi grown in submerged culture are significantly different from the conditions these same cells were exposed to on each polymer coating; but submerged growth data does provide a straightforward comparison for any unusual growth activity resulting from polymer degradation by these fungi. In comparison to the *Fungus 2* and *Fungus 1*, our growth data indicates that *Fungus 3* and *Fungus 4* have developed a more self-sufficient approach to survival on these atypical carbon sources. These data also suggest that *Fungus 3* and *Fungus 4* will use indirect mechanisms to degrade the polymer surfaces. This second trend addresses a key hurdle for the program since up until this point we had collected minimal direct evidence that any of these fungi used different metabolic pathways while degrading the polymers.

Darby and Kaplan performed a similar type of growth survey in 1968 using a consortium of fungi with many of the same diols and carboxylic acids (Darby and Kaplan, 1968). Their results showed that their consortium of fungi grew on 1,4-butanediol, 1,5-pentanediol, and 1,6-hexanediol and degraded the corresponding polymers synthesized with those diols suggesting that unbranched carbon chains were more susceptible to enzymatic attack than branched. The hydrolysis of Irogran[®] would liberate the unbranched 1,4-butanediol and PES and PEA will liberate monoethylene glycol. The vapor pressures of 1,4-butanediol and monoethylene glycol are 0.011 mm Hg and 0.060 mm Hg, respectively at 25°C (Rumble, 2018) making observing them as a degradation product possible but their concentration might be so low that it would be below the detection limits. Neither *Fungus 1* nor *Fungus 2* utilized ethylene glycol for planktonic growth but *N. albida* did show some marginal growth using 1,4-butanediol and 1,6-hexanediol at pH 5.5.

As for the succinic and adipic acids, the planktonic growth results in **Figure 16** are consistent with growth observed on PEA and PES coatings by *Fungus 1* in **Figure 6** and **Figure 8**, respectively. Succinate is a key intermediate in the tricarboxylic acid (TCA) cycle and these data support the growth of *Fungus 1* on the PES coatings and the extent of the degradation that occurred (**Figure 9**). The fact that this strain of *Fungus 2* does not use succinate as an external supplemental carbon source for planktonic growth suggests that it cannot actively uptake succinate though other isolates of *Fungus 2* can grow using compounds like glutamic acid (Tang and Howard, 1973). PES can be degraded and results in the growth of *Fungus 1* under identical degradation conditions and in comparison to the *Fungus 2* these results correlate how little activity was observed on PES from *Fungus 2* (**Figure 9**). However, this same type of correlation cannot be made for each of these fungal strains with adipate and PEA.

The data presented in **Figure 7** and the time-dependent phase contrast images (**Figure 6**) of the biodegradation of PEA coatings after 8 days showed significant growth and removal of the coating by *Fungus 1* and the highest degree of degradation using *Fungus 2* of all the coatings. Thus, we expected adipate to be a viable carbon source for growth from the data shown in **Figure 16**. These data indicate that not only is adipate a viable carbon source for biofilm growth by both fungi but adipate is stimulating hydrolysis of PEA. The degradation patterns that we observed using all of the coatings suggests that degradation occurs over the entire area of the original spot and as the coating is removed the areas of the most rapid degradation are potentially directed toward deeper regions of the coating.

We used the growth of each fungi as planktonic cultures to determine if the carbon sources liberated from the coating are viable carbon sources for the growth that we observed on the polymers. Collectively, the microscopy data indicate that biofilms of both fungi generated viable carbon sources with the trend in activity as follows: PEA>> PES> Irogran[®]. *Fungus 1* was more active than *Fungus 2* on all polymers and is consistent with its increased growth density over the same period of time on aliphatic compounds such as 1,3-diaminopropane and succinate.

As biofilms, the cells were metabolically active but not spreading over the surface as they metabolized the Irogran[®] hydrolysis products but were spreading over the surface of PEA

coatings in particular. Neither of these strains are motile, so movement on the polymer surface would be due to replication or surface water. The combination of our biodegradation results using these three polymers with biofilms of these yeasts and their growth as planktonic cultures suggests that these strains are secreting active hydrolases early in the degradation process but becoming deactivated over a period of 7 days. More specifically, the cells are degrading the polymer to survive on the surface and can completely oxidize the polymer degradation products but polymers with significantly less liberated carbon sources reduces the growth of the yeasts. These experiments are consistent with mirroring conditions experienced by fungi at the early stages of the biofouling which are some of the most important periods for evaluating biodegradation processes and their potential impact on the environment.

Fungus 1 single Cell AFM-IR degradation Experiments on Irogran®

Figure 17 shows a pair of optical images (top) of a *Fungus 1* biofilm on an Irogran film used for AFM-IR analysis. The images show the biofilms at 24 hours and after 25 days at 25°C and 100% humidity. The dark regions are covered with monolayer clusters of cells, which was confirmed by AFM. The green-yellow-blue-purple coloring is due to light interference in the PU film, which had some quasi-periodic thickness variation of about 20 nm (greenish-yellow is at the peaks and troughs; blue – purple is intermediate). Over the 25 day period, growth and position changes of cells can be observed. The two circles at region “A” serve as fiducial markers where only minor change occurred. The circled regions at “B” are examples where significant changes occurred, including increased surface coverage of cells, and cell movement (presumably through non-motile mechanisms). Changes in coating thickness near the biofilm are also apparent by subtle changes in color. Also note the faint particle formations at the outer perimeter of the biofilm at day 25.

The lower images in **Figure 17** show examples of the corresponding AFM images, confirming the monolayer cell clusters composing the biofilms in the optical images. The images also show interesting cell morphological variations at the 24 hour time point, including “deflated” and “rounded” appearances. Time dependent changes are also observable at the 25 day time point shown to the right. Circled regions highlight examples for direct comparison. Region 1 shows two cells at 24 hours and an additional “bump” at day 25.

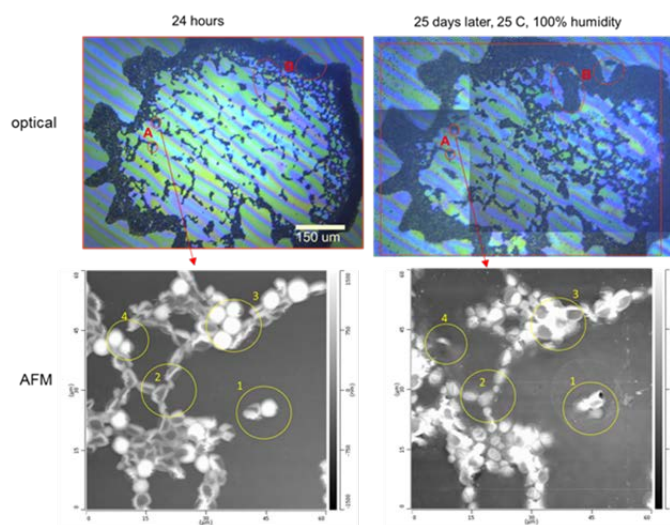


Figure 17 (Top) Optical images of a *Fungus 1* biofilm on an Irogran® film used for AFM-IR analysis. The images show the biofilms at 24 hours and after 25 days at 25°C and 100% relative humidity. (Bottom) AFM imaging showing changes occurring at the single cell level.

Region 2 shows “deflated” cells at 24 hours with more rounded appearance at day 25. Region 3 shows four distinguishable, highly rounded cells at 24 hours where at 25 days the cluster is less distinguishable except for three cells that had lost their structural integrity. Region four shows two rounded cells at 24 hours that are non-existent at 25 days. These changes help confirm cell activity in the absence of cell viability which was also supported by the measurement of CO₂ in the headspace from sealed degradation reactions. They are also indicative of heterogeneity in individual cell physiology at given time points, and changes in physiology as time progresses.

Under ambient conditions, AFM showed that cells were well-adhered to the polymer raising questions of how cell movement may occur. While yeast cells are non-motile, they can spread through division. We also hypothesize that the cell movement observed in Figure 2 may occur under high humidity when water condenses on the surface. Condensed water could lower cell adhesion to the surface and enable potential mechanisms for induced surface movement. Future environmental AFM experiments are planned to investigate the role of water as was proposed in this program in Task 4 since clearly condensed water may also aid in the dispersal of the nanoparticles observed around the biofilm at day 25.

Heterogeneous PU degradation at the single / multi - cellular levels with yeast cells

Figure 18a-c shows corresponding topography and IR images of cells on the Irogran[®] film over a region expanded from the AFM images shown in **Figure 17**. The biomaterial map (**Figure 18b**) shows clear contrast associated with cells, and that some particles in the topography image are not biomaterial associated. The PU degradation map also indicates varying degrees of degradation underneath the larger cell clusters, with some single cells having noticeably higher degradation than other cells. The boxed region identifies one such case and is shown in greater detail in **Figure 18d-f**. Here, near the center of the PU degradation image, we can see a particularly dark spot, indicating higher local degradation. The biomaterial and topography maps show correlation with the presence of a cell. This location also correlates with a feature showing similarity to a budding yeast cell. The topography in this region shows local depressions, indicating that the region could reflect a cell sitting in a degradation produced depression in the polymer. The depressions and central “bump” (that is likely a cell) are also shown by the line profile in **Figure 18g**. **Figure 18h** shows examples of single point infrared spectra that were acquired at points A and B in **Figure 18f** and also identifies the 1732 cm⁻¹ and 1536 cm⁻¹ peaks used to produce the PU degradation maps. For pristine Irogran films, the 1732 cm⁻¹ / 1536 cm⁻¹ peak ratio (based on the IR laser alignment used for this work) was 4.8 +/- 0.2. Here, the ratio indicates significant degradation through preferential ester loss at point A

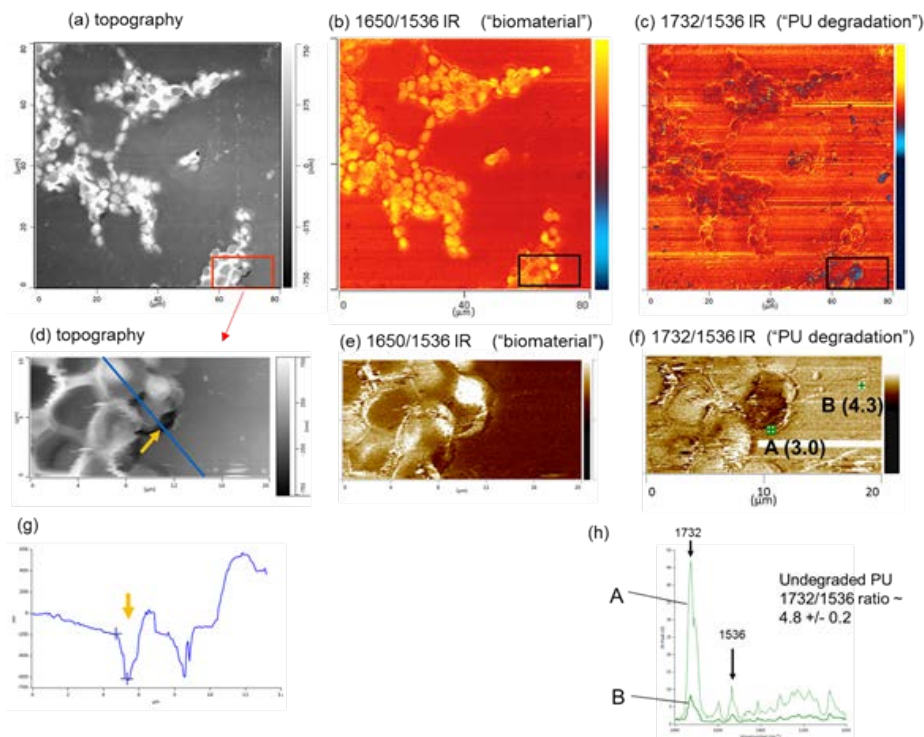


Figure 18 AFM-IR imaging showing varying local PU degradation by *Fungus I* after 25 days at RH% = 100

with a ratio of 3.0 and much lower levels of degradation also likely at point B. The overall difference in peak intensities at points A and B also indicates bulk polymer loss at point A, consistent with the topography image. **Figure 19** shows a similar analysis of single cells with high local degradation.

Another type of localized degradative feature that was observed was cracking at edges of cell clusters. An example is shown in the topography image in **Figure 20a**, which shows a crack at the edge of the cell cluster. The PU degradation image in **Figure 20c** shows that this is not simply a stress crack since higher preferential ester loss is localized in the vicinity of the crack. The image also indicates more uniform PU degradation underneath the cell cluster. **Figure 20d-f** also show a degradation associated crack at location C, but under more complex conditions. Cells clusters can be identified corresponding to point D in the topography and biomaterial images, but lower levels of biomaterial are also detectable in the region and then for reasons currently unknown there was either a movement or decay of cells with some biomaterial left behind. Region B shows a smoother morphology than the opposite side of the crack indicating that this region may not have been covered by cells, but may have been coated with secretions from the cells. The topography shows a step going from region A to B, indicating that region B is covered with some kind of film, as well as the region on the lower left of the crack extending to the cell clusters. This film may be extracellular polymeric substances (EPS) produced by the biofilm that remained adhered after cell removal by whatever mechanism.

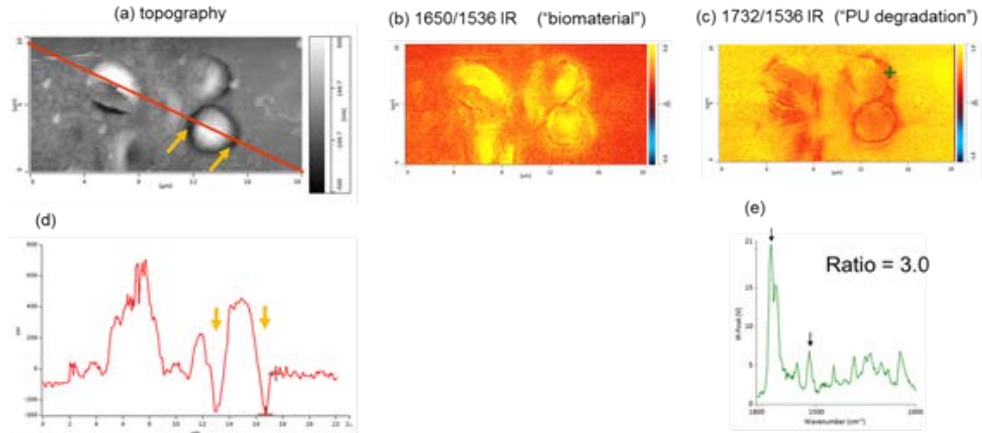


Figure 19 Additional high PU degradation localized at single cells. 25 day time point.

These results show that the early stage of degradation processes among individual cells and cell clusters is varied and complex. This could be due to varying physiology which could result in the local variation of chemical environment and / or enzyme secretion. Local variation in chemical environment could also impact enzyme activity. We have observed heterogeneous polyurethane degradation in other work in the form of pitting (Nadeau et al., 2018) and have hypothesized that local changes in chemical environment from enzymatic hydrolysis could provide positive feedback enhancing enzyme activity and further increasing the rate of degradation. Future research efforts will involve further elucidation of chemical environment, such as pH, the impacts on enzymatic activity, and relationships to cell physiology.

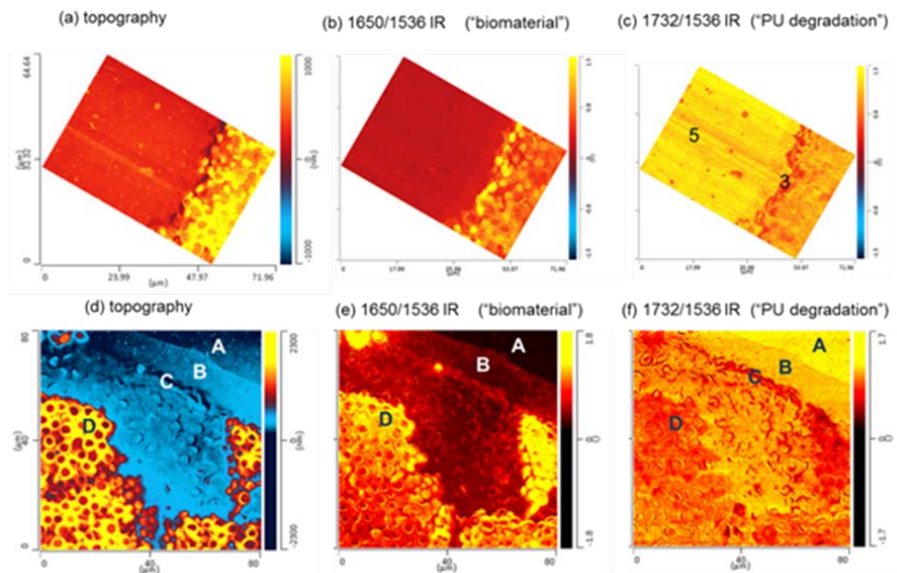


Figure 20 Localized degradative cracking and additional changes. (30 day time point.)

Mineralization of Polymers using *Fungus 3* and *Fungus 4*

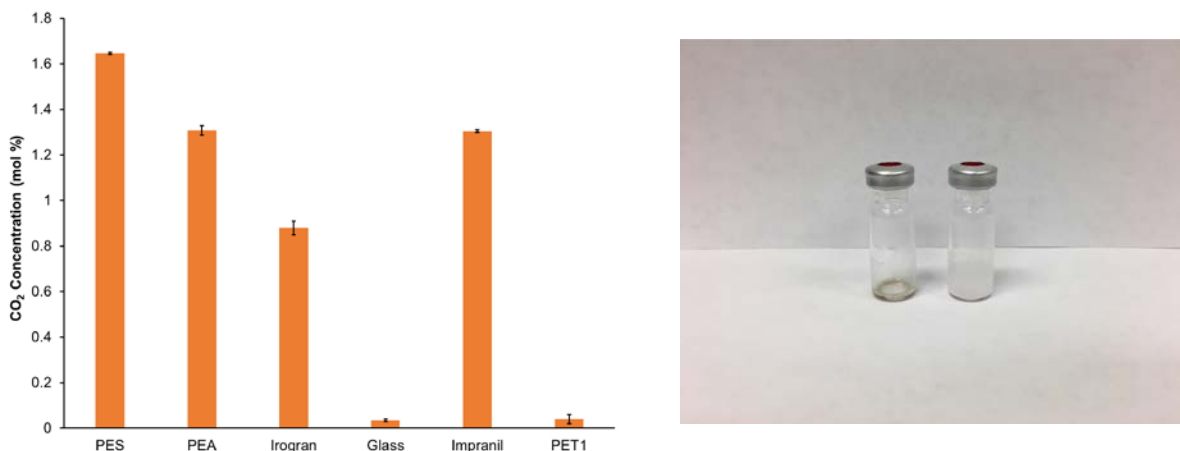


Figure 21 Comparison of the concentration of CO₂ generated by *Fungus 3* after 336 h on all polymers and an image of the degradation of Irogran[®] (left vial) by *Fungus 3* compared to the control vial with Irogran[®]. PES: Polyethylene succinate, PEA: Polyethylene adipate, Glass (control experiment with cells and no polymer).

Fungus 3 generated significantly more CO₂ (>40%) than either *Fungus 4* or either yeast strain. There were also data supporting that *Fungus 3* degraded Irogran[®] more aggressively than either yeast strain, based on the CO₂ production (**Figure 21**) and microscopy data from the degradation of PEA (**Figure 22**) and on Irogran[®] (**Figure 23**) at RH%: 100. These data are the first evidence that *Fungus 3* is an active Irogran[®] degrader and that the degree of degradation using this strain will affect a larger surface area of the polymer than the non-motile yeasts. We are currently working on determining if this fungus is spreading over the surface of the polymer as a reason for the elevated production of CO₂. Our microscopy data shows that *Fungus 3* is propagating over the surface passed the boarder of the original cell spot. This fungus also generates a comparable quantity of CO₂ from Irogran[®] or polyethylene adipate unlike the yeasts. These results are direct evidence that this fungus is using the adipate hydrolysis product while the cells are degrading Irogran[®] and is an opportunity to create the first comparative model between the degradation of the same polymers with two distinct morphologies and transmission mechanisms. We will use these data in conjunction with IR mapping results to confirm both the cell morphology and the location of the degradation products relative to this cell type. Thus far, our data supports that *Fungus 3* is using a direct polymer degradation mechanism thus far.

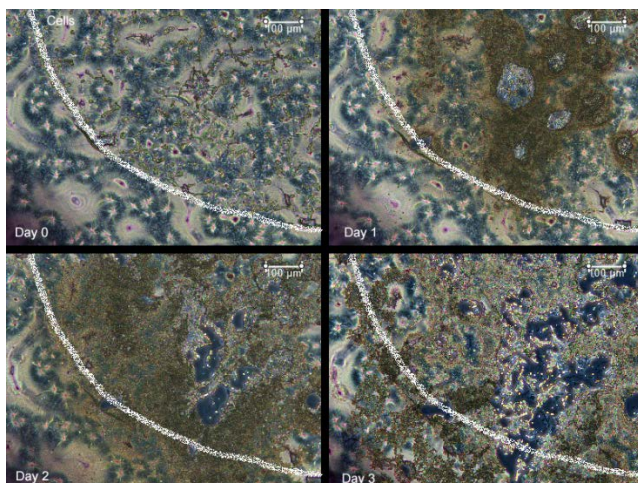


Figure 22 Selected time-dependent phase contrast (Phase I) optical microscopy images of a region of a Polyethylene adipate coating exposed to *Fungus 3* over 3 days of exposure at RH: 100%.¹¹

The prospects of *Fungus 3* being a more active and prolific degrader of synthetic polymers are high. This observation is based on both the high metabolic output of CO₂ and the level of degradation observed on Irogran® (**Figure 21**) and PEA coatings (**Figure 22**) and Irogran coatings (**Figure 23**) using phase contrast microscopy. Not only was the rate of the complete degradation of PEA higher than *Fungus 1* by 40% but also significant pitting was observed on Irogran® coatings around the hyphal structures in addition to localized sporulation. Our proof of concept results with *Fungus 3* thus far shows that we have a viable fungal species to compare with the degradation behavior from both yeasts

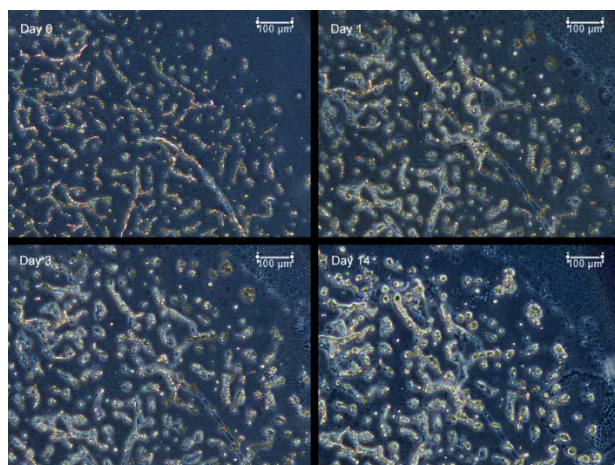


Figure 23 Selected time-dependent phase contrast (Phase I) optical microscopy images of a region of a Irogran® coating exposed to *Fungus 3* over 14 days of exposure at RH: 100%.

¹¹ White lines were rendered onto the image to highlight the boundary between where the cells were originally drop cast and unexposed polymer .

Fungus 4

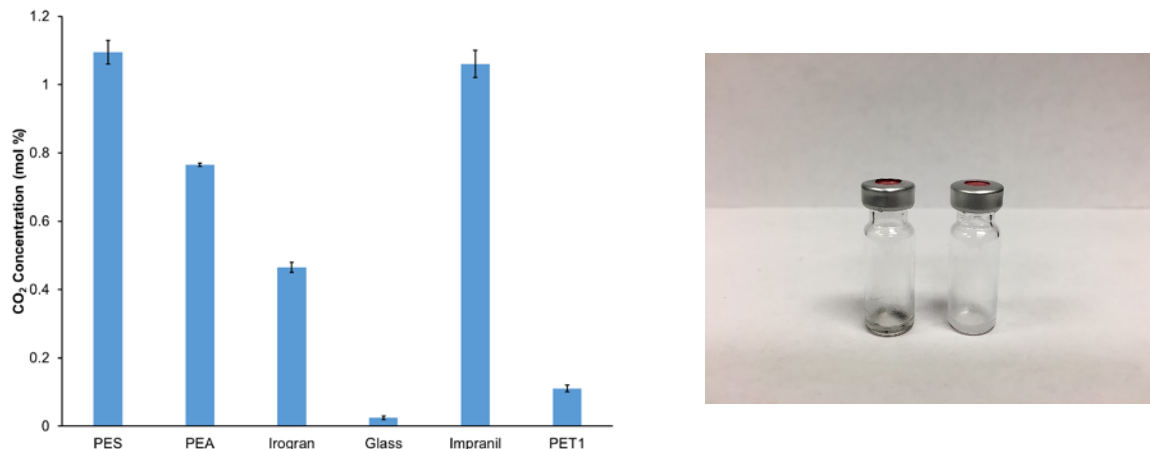


Figure 24 Comparison of the concentration of CO₂ generated by *Fungus 4* after 336 h on all polymers and an image of the degradation of Irogran (left vial) by *Fungus 4* compared to the control vial with Irogran. PES: Polyethylene succinate, PEA: Polyethylene adipate, Glass (control experiment with cells and no polymer)

Fungus 4 was the last fungus to be studied by our team in sealed gas phase experiments. The images of the vials containing the polymer show the growth of the fungus in these sealed experiments on Irogran® in addition to reaching a sporulation state (indicated by the black color of the fungal masses) after 7 days. We also observed significant degradation of Irogran® visually in these vials (**Figure 24**). The amount of CO₂ generated was less (approx. 20%) over the same time frame as *Fungus 3* based on the degradation of Irogran. However, *Fungus 4* is the only organism so far that has shown any activity on PET1 (**Figure 24**; polyether polyurethane coating) which presents a large opportunity for the program to understand how this particular organism is interacting and degrading a polyether polyurethane topcoat that has yet to be degraded by any other microorganism we have studied over the last 8+ years.

Conclusions and Implications for Future Research

At the beginning of the SEED effort we isolated and identified four fungal strains that were able to clear the colloidal polyester polyurethane Impranil®. Using these strains we have identified two different mechanisms for the degradation of polyester polyurethanes by non-motile yeasts and identified the importance of water in the degradation process. One of the major risks in our initial effort was that, because we conducted our screen using Impranil, we had selected for fungi that were ONLY active Impranil® degraders. But that was not the case as we have now reproducibly degraded polyesters and polyester polyurethanes. In addition, our baseline data for the degradation of polymer surfaces using *Fungus 1* and *Fungus 2* and the preliminary data for fungal basidiomycetes confirm that we will be able to make fundamental comparisons between different fungal classes and genera in future research efforts. The many successes we encountered in this SEED program have led to areas that we consider opportunities for future efforts.

By creating control coatings around known polymers we will continue to build on the active and aggressive degradation data we have already collected using the unmodified polymers as well as introduce ^{13}C -labeling within the polyester backbone without changing the polymer coating completely. ^{13}C -labeled polymers will be used to determine the biological fate of the hydrolysis products which is not part of the current SEED effort but aid in identifying how the polymer is being metabolized. The use of non-motile yeast streamlined our analysis in the SEED program but we expect significant difficulty in determining how fungal morphology is impacting degradation with a cell type that can generate different cellular structures (like *Fungus 3* and *Fungus 4*) during the degradation of the polymer.

Literature Cited

- Bester E, Kroukamp O, Wolfaardt GM, Boonzaaier L, Liss SN. Metabolic Differentiation in Biofilms as Indicated by Carbon Dioxide Production Rates. *Applied and Environmental Microbiology* 2010; 76: 1189-1197.
- Bierwagen GP, Tallman DE. Choice and measurement of crucial aircraft coatings system properties. *Progress in Organic Coatings* 2001; 41: 201-216.
- Biffinger JC, Barlow DE, Pirlo RK, Babson DM, Fitzgerald LA, Zingarelli S, et al. A direct quantitative agar-plate based assay for analysis of *Pseudomonas protegens* Pf-5 degradation of polyurethane films. *International Biodeterioration and Biodegradation* 2014; 95: 311-319.
- Chen K-S, Leon Yu T, Chen Y-S, Lin T-L, Liu W-J. Soft-and hard-segment phase segregation of polyester-based polyurethane. *Journal of Polymer Research* 2001; 8: 99-109.
- Christenson EM, Anderson JM, Hittner A. Biodegradation mechanisms of polyurethane elastomers. *Corrosion Engineering Science and Technology* 2007; 42: 312-323.
- Cortes-Tolalpa L, Salles JF, van Elsas JD. Bacterial Synergism in Lignocellulose Biomass Degradation - Complementary Roles of Degraders As Influenced by Complexity of the Carbon Source. *Frontiers in Microbiology* 2017; 8: 14.
- Cosgrove L, McGeechan PL, Robson GD, Handley PS. Fungal communities associated with degradation of polyester polyurethane in soil. *Applied and Environmental Microbiology* 2007; 73: 5817-5824.
- Da Luz JMR, Paes SA, Ribeiro KVG, Mendes IR, Kasuya MCM. Degradation of green polyethylene by *Pleurotus ostreatus*. *PLoS ONE* 2015; 10.
- da Silva RR, Peduzzi R, Souto TB. Exploring the bioprospecting and biotechnological potential of white-rot and anaerobic Neocallimastigomycota fungi: peptidases, esterases, and lignocellulolytic enzymes. *Applied Microbiology and Biotechnology* 2017; 101: 3089-3101.
- Darby RT, Kaplan AM. Fungal Susceptibility of Polyurethanes. *Applied and Environmental Microbiology* 1968; 16: 900-905.
- Ishii N, Inoue Y, Shimada Ki, Tezuka Y, Mitomo H, Kasuya Ki. Fungal degradation of poly(ethylene succinate). *Polymer Degradation and Stability* 2007; 92: 44-52.
- Keller NP, Turner G. Fungal Secondary Metabolism. *Methods in Molecular Biology* (Book 944). Humana Press, New York City, NY, 2013, pp. 288.

- Kiegler-Böckler G. Specifications and Testing in Automotive Paints and Coatings. Weinheim: Wiley-VCH, 2008.
- Kim DY, Rhee YH. Biodegradation of microbial and synthetic polyesters by fungi. *Applied Microbiology and Biotechnology* 2003; 61: 300-308.
- Krueger MC, Harms H, Schlosser D. Prospects for microbiological solutions to environmental pollution with plastics. *Applied Microbiology and Biotechnology* 2015; 99: 8857-8874.
- Kumar Sen S, Raut S. Microbial degradation of low density polyethylene (LDPE): A review. *Journal of Environmental Chemical Engineering* 2015; 3: 462-473.
- Lara CA, Santos RO, Cadete RM, Ferreira C, Marques S, Gírio F, et al. Identification and characterisation of xylanolytic yeasts isolated from decaying wood and sugarcane bagasse in Brazil. *Antonie van Leeuwenhoek, International Journal of General and Molecular Microbiology* 2014; 105: 1107-1119.
- Liu XZ, Wang QM, Theelen B, Groenewald M, Bai FY, Boekhout T. Phylogeny of tremellomycetous yeasts and related dimorphic and filamentous basidiomycetes reconstructed from multiple gene sequence analyses. *Studies in Mycology* 2015: 1-26.
- Loredo-Treviño A, Gutiérrez-Sánchez G, Rodríguez-Herrera R, Aguilar CN. Microbial Enzymes Involved in Polyurethane Biodegradation: A Review. *Journal of Polymers and the Environment* 2012; 20: 258-265.
- Mahajan N, Gupta P. New insights into the microbial degradation of polyurethanes. *RSC Advances* 2015; 5: 41839-41854.
- May RC, Stone NRH, Wiesner DL, Bicanic T, Nielsen K. Cryptococcus: From environmental saprophyte to global pathogen. *Nature Reviews Microbiology* 2016; 14: 106-117.
- Nadeau L, Barlow DE, Hung C-S, Biffinger JC, Crouch AL, Russell Jr. JN, et al. Polyurethane Coating Deterioration by Unsaturated Biofilms of *Pseudomonas protegens* Pf-5: The Impacts of PueA and PueB Hydrolases. *Science of the Total Environment* 2018.
- Oberbeckmann S, Osborn AM, Duhaime MB. Microbes on a bottle: Substrate, season and geography influence community composition of microbes colonizing marine plastic debris. *PLoS ONE* 2016; 11.
- Paço A, Duarte K, da Costa JP, Santos PSM, Pereira R, Pereira ME, et al. Biodegradation of polyethylene microplastics by the marine fungus *Zalerion maritimum*. *Science of the Total Environment* 2017; 586: 10-15.
- Powers DS, Vaia RA, Koerner H, Serres J, Mirau PA. NMR characterization of low hard segment thermoplastic polyurethane/carbon nanofiber composites. *Macromolecules* 2008; 41: 4290-4295.
- Restrepo-Flórez JM, Bassi A, Thompson MR. Microbial degradation and deterioration of polyethylene - A review. *International Biodeterioration and Biodegradation* 2014; 88: 83-90.
- Rumble JR. *CRC Handbook of Chemistry and Physics*. CRC Press/Taylor & Francis, Boca Raton, FL, 2018, pp. Internet Version 2018.
- Sambrook J, Russell DW. *Molecular Cloning: A Laboratory Manual*. Vol 3. New York: Cold Spring Harbor Laboratory Press, 2001.
- Shah AA, Hasan F, Hameed A, Ahmed S. Biological degradation of plastics: A comprehensive review. *Biotechnology Advances* 2008; 26: 246-265.
- Shah AA, Kato S, Shintani N, Kamini NR, Nakajima-Kambe T. Microbial degradation of aliphatic and aliphatic-aromatic co-polyesters. *Applied Microbiology and Biotechnology* 2014; 98: 3437-3447.

- Smirnou D, Krčmář M, Kulhánek J, Hermannová M, Bobková L, Franke L, et al. Characterization of Hyaluronan-Degrading Enzymes from Yeasts. *Applied Biochemistry and Biotechnology* 2015; 177: 700-712.
- Stone W, Kroukamp O, Korber DR, McKelvie J, Wolfaardt GM. Microbes at surface-air interfaces: The metabolic harnessing of relative humidity, surface hygroscopicity, and oligotrophy for resilience. *Frontiers in Microbiology* 2016a; 7.
- Stone W, Kroukamp O, Moes A, McKelvie J, Korber DR, Wolfaardt GM. Measuring microbial metabolism in atypical environments: Bentonite in used nuclear fuel storage. *Journal of Microbiological Methods* 2016b; 120: 79-90.
- Szycher M. *Szycher's Handbook of Polyurethanes*. Boca Raton, FL: CRC Press, 2013.
- Tang SL, Howard DH. Uptake and utilization of glutamic acid by *Cryptococcus albidus*. *Journal of Bacteriology* 1973; 115: 98-106.
- Varjani SJ, Upasani VN. A new look on factors affecting microbial degradation of petroleum hydrocarbon pollutants. *International Biodeterioration and Biodegradation* 2017; 120: 71-83.
- Zafar U, Houlden A, Robson GD. Fungal communities associated with the biodegradation of polyester polyurethane buried under compost at different temperatures. *Applied and Environmental Microbiology* 2013; 79: 7313-7324.

Appendix

Supporting Figures

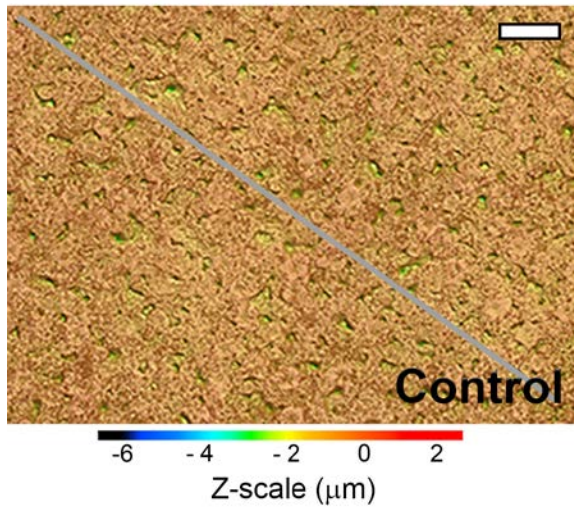


Figure S1 Confocal Microscopy Image of region of PEA coating exposed initially to sterile water after 8 days. White scale bars are 100 μm.

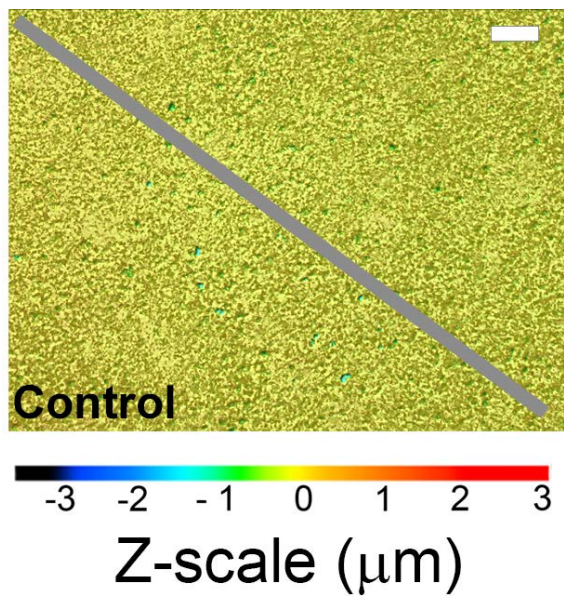


Figure S2 Confocal Microscopy Image of region of PES coating exposed initially to sterile water after 8 days. White scale bars are 100 μm.

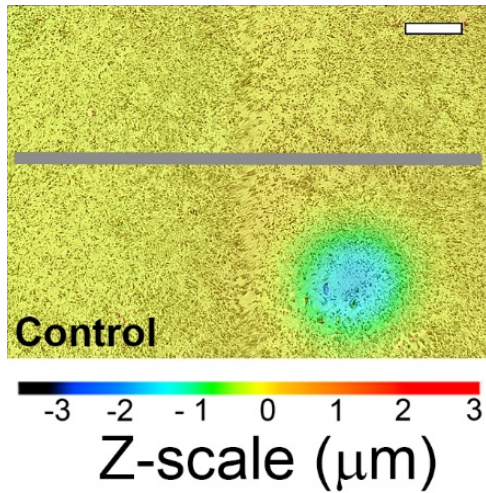


Figure S3 Confocal Microscopy Image of region of an Irogran® coating exposed initially to sterile water after 8 days. White scale bars are 100 μm .

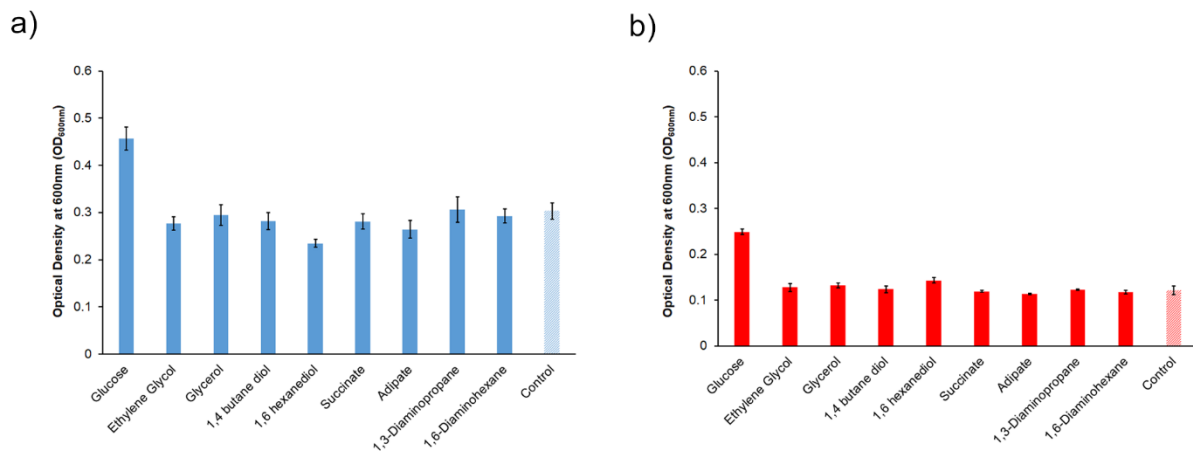


Figure S4 Growth of a) *Fungus 1* and b) *Fungus 2* in a 1:10 dilution of Tryptic Soy Broth (TSB) media with 10mM of each carbon source over 48 hours at 25°C. Growth experiments were performed in triplicate from cell suspensions with an OD_{600nm} of 0.6 ± 0.1 . Control growth experiments contained only 1:10 TSB/water.